CHOICE OF SENSOR LOCATIONS AND VIBRATION CONTROL IN FLEXIBLE HELICOPTER FUSELAGE SYSTEM

by

A. UDAYASANKAR

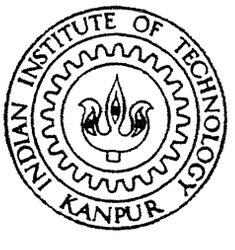

DEPARTMENT OF AEROSPACE ENGINEERING

INDIAN INSTITUTE OF TECHNOLOGY KANPUR

MARCH, 1997

CHOICE OF SENSOR LOCATIONS AND VIBRATION CONTROL IN FLEXIBLE HELICOPTER FUSELAGE SYSTEM

A thesis submitted

in partial fulfillment of the requirements

for the degree of

MASTER OF TECHNOLOGY

by

A. UDAYASANKAR

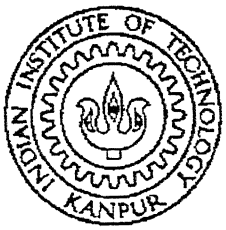

DEPARTMENT OF AEROSPACE ENGINEERING
INDIAN INSTITUTE OF TECHNOLOGY, KANPUR

March, 1997

AE-1997-M-UDA-CHO

CERTIFICATE

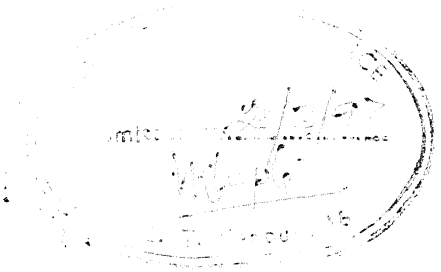

Certified that the work contained in this thesis entitled "**CHOICE OF SENSOR LOCATIONS AND VIBRATION CONTROL IN FLEXIBLE HELICOPTER FUSELAGE SYSTEM** ", by **A. UDAYASANKAR**, has been carried out under my supervision and that this work has not been submitted elsewhere for a degree.

19, March, 1997

Dr. C. VENKATESAN
Department of Aerospace Engineering
Indian Institute of Technology
Kanpur

DEDICATED

TO

MY PARENTS

ACkNOWLEDGEMENTS

I express my deep gratitude and indebtedness to Dr. C. Venkatesan for his guidance and suggestions throughout my thesis work.

My sincere thanks are due to Guppi, Gomes and Kalyan who helped me during the computer programming part of the thesis. I would like to thank Saravanan, Navaneet, Kali, Siva and Joye for their encouragement and help throughout this work.

Finally, I would like to thank all the persons who helped me directly or indirectly during my thesis work.

Contents

List of Figures

List of Tables

ABSTRACT

Vibration control has always been a challenging problem to the helicopter designer. The present study addresses the problem on the formulation and solution of an active vibration control scheme in helicopters, based on the new concept of Active Control of Structural Response (ACSR). First, using a mathematical procedure employing Fisher Information Matrix, the optimum sensor locations for vibration measurement in a three dimensional flexible fuselage have been identified. It is observed that irrespective of the excitation frequency, these optimally selected sensor locations experience relatively high levels of vibration. Then, using the measurement from these optimal sensor locations, a Multi-Input-Multi-Output (MIMO) control problem has been formulated and solved to obtain the active control forces required for vibration minimisation in the helicopter fuselage.

NOMENCLATURE

[A], [B], [C]	System matrix, control matrix and output matrix respectively
C_i	Damping of the i-th gearbox mounting
$[C]_s$	Output matrix defined for preselected sensor locations
E	Idempotent matrix
$\{F_{Hx}, F_{Hy}, F_{Hz}\}$	Hub shears in the nonrotating hub fixed coordinate system
$\{F^k{}_{xR}, F^k{}_{yR}, F^k{}_{zR}\}$	Root shears of the k-th blade in the hub fixed rotating coordinate system
$\{F_{xi}, F_{yi}, F_{zi}\}_{GB}$	Force vector due to the i-th gearbox mounting
$\{F_{xi}, F_{yi}, F_{zi}\}_C$	Control force vector at the i-th gearbox mounting
$\{F_x, F_y, F_z\}_{Hub}$	Forces acting on the gearbox at the rotor hub
$\{F_x, F_y, F_z\}_{gravity}$	Gravitational force vector
$\{F_x, F_y, F_z\}_{GB}$	Resultant force vector on the gearbox
$\{F_x, F_y, F_z\}_F$	Resultant force vector on the fuselage
$\{F_x, F_y, F_z\}_{Aerodynamic}$	Aerodynamic force vector on the fuselage
$\{F_x, F_y, F_z\}_{Tail}$	Tail rotor forces acting on the fuselage
$\{F_{xm}, F_{ym}, F_{zm}\}_F$	Resultant mean forces acting on the fuselage
$\{F_{xm}, F_{ym}, F_{zm}\}_{GB}$	Mean force vector acting on the gearbox
$\{f\}$	Forcing vector
$\{H_x, H_y, H_z\}$	Radius vector from the gearbox centre of mass to rotor hub

$\{h_{xi}, h_{yi}, h_{zi}\}$	Radius vector from fuselage centre of mass to i-th mounting of the gearbox
$\{h_{xT}, h_{yT}, h_{zT}\}$	Radius vector from fuselage centre of mass to tail rotor force vector
$\{I_{xx}, I_{yy}, I_{zz}, I_{xy}, I_{yz}, I_{zx}\}_{GB}$	Mass moment of inertia of gearbox
$\{I_{xx}, I_{yy}, I_{zz}, I_{xy}, I_{yz}, I_{zx}\}_{F}$	Mass moment of inertia of fuselage
K_i, K^i	Stiffness of the i-th gearbox mounting
(l, m, n)	Direction cosines of the i-th gearbox mounting
$\tilde{M}$	Moment vector
$\tilde{M}_m$	Mean value of moment vector
M_A	Number of available sensors
M_L	Initial number of candidate sensor locations
$[M]_b, [C]_b, [K]_b$	Mass, damping and stiffness matrices of the rotor blade
$\{M_x, M_y, M_z\}$	Hub moments in the hub fixed nonrotating coordinate system
$\{M_{Hx}, M_{Hy}, M_{Hz}\}$	Hub moments in the hub fixed nonrotating coordinate system
$\{M^k{}_{xR}, M^k{}_{yR}, M^k{}_{zR}\}$	Root moments of the k-th blade in the hub fixed rotating coordinate system
$\{M_x, M_y, M_z\}_{GB}$	Resultant moment about the gearbox centre of mass
$\{M_x, M_y, M_z\}_{Hub}$	Moment vector on the gearbox applied at the rotor hub

$\{M_x, M_y, M_z\}_F$	Resultant moment about the fuselage centre of mass
$\{M_x, M_y, M_z\}_{Aerodynamic}$	Aerodynamic moment about the fuselage centre of mass
$\{M_x, M_y, M_z\}_{Tail}$	Moment due to tail rotor
$\{M_{xm}, M_{ym}, M_{zm}\}_F$	Resultant mean moment about the fuselage centre of mass
$[M]_F, [C]_F, [K]_F$	Mass, damping and stiffness matrices of the fuselage in finite elment domain
$[\bar{M}], [\bar{C}], [\bar{K}]$	Modal mass, damping and stiffness matrices respectively
m_B	Rotor blade mass
m_F	Mass of fuselage
m_{GB}	Mass of gearbox
NB	Number of blades in the rotor system
Nm	Number of flexible modes of the fuselage
$\{p_{xi}, p_{yi}, p_{zi}\}$	Radius vector from the gearbox centre of mass to the i-th gearbox mounting
$\{\eta\}$	Modal coordinate vector
$\{\hat{\eta}\}$	Estimate of the states of the system
$\{Q\}_F$	Generalised force vector
$Q^j{}_F$	Generalised force for the j-th vibrational mode of the fuselage
$\{q\}$	State vector
R	Rotor radius
$\{R_{Hx}, R_{Hy}, R_{Hz}\}$	Perturbational translation of the hub
$\{U\}$	Control force vecor
$\{x_i, y_i, z_i\}_{GB}$	Displacement vector of point I (see Fig.1)
$\{x_i, y_i, z_i\}_F$	Displacement vector of point I' (see Fig.1)

$\{x_{GB}, y_{GB}, z_{GB}\}$	Displacement vector of the gearbox centre of mass
$\{x_F, y_F, z_F\}$	Displacement vector of the fuselage centre of mass
$\{Y_s\}$	Vibratory response at preselected sensor locations
$\{y\}$	Output vector or generalised coordinate vector
β	Structural damping coefficient
$[\Phi_s]$	Modal matrix corresponding to the initial set of candidate sensor locations
$\{\Psi^i_{jx}, \Psi^i_{jy}, \Psi^i_{jz}\}$	Modal displacement in j-th mode of the fuselage at i-th gearbox mounting
ψ_k	Azimuthal position of the k-th blade
$\{\theta_{xGB}, \theta_{yGB}, \theta_{zGB}\}$	Angular displacement of the gearbox
$\{\Theta_{Hx}, \Theta_{Hy}, \Theta_{Hz}\}$	Angular displacement of the hub
$\{\theta_{xF}, \theta_{yF}, \theta_{zF}\}$	Angular displacement of the fuselage
Ω	Rotor angular velocity
$\{\ \}_{GB}$, $[\ ]_{GB}$	Quantities corresponding to gearbox
$\{\ \}_F$, $[\ ]_F$	Quantities corresponding to fuselage

Publications based on this thesis

1. 'Choice ofmeasurementlocations for active vibration control in helicopters', Accepted for presentation at the Confederation of European Aerospace Societies(CEAS) International Forum on Aeroelasticity and Structural Dynamics, June 17-20, 1997, Rome.

2. 'Sensor locations and active vibration control in helicopters', Submitted to 23-rd European Rotorcraft Forum, Sept. 1997, Germany.

Chapter 1

INTRODUCTION

During forward flight, the time dependent aerodynamic and inertia loads acting on the rotor blades cause vibration in helicopters. These rotor loads are transmitted to different parts of the fuselage through a complicated load path and cause discomfort to pilot and crew, equipment deterioration, fatigue damage to the structure and increased maintenance cost. As a result, these vibratory loads restrict the operation and efficiency of the vehicle. With increasing demand for high speed and high performance helicopters, vibration control has become an important objective in the design of modern helicopters. References 1-3 provide excellent review of helicopter vibration and its control.

Over the years, the vibratory levels in the fuselage of the helicopters have been reduced by using passive vibration control devices and/ or by suitable structural design. For present day helicopters, the general requirement is to have a maximum vibratory level of 0.1g in the fuselage. However, in future, with the adoption of stringent vibration control, it will become necessary to reduce the vibratory levels below 0.05g or even 0.02g (Ref.4). In recent years, a substantial amount of research and development effort has been made at vibration prediction and reduction methodologies in helicopters and also at improving

the fundamental understanding of the dynamics of the coupled rotor - fuselage helicopter systems.

The various vibration control schemes adopted in helicopters can be classified as either passive or active control methodologies. Since the major cause of vibration in helicopters is the main rotor, one of the passive methods of reducing vibration is to carefully design the rotor hub and blades (Ref.5). Since the rotor design is based on a compromise between a number of conflicting aeroelastic, aeromechanical stabilities, performance and handling quality requirements, vibration reduction solely by a proper design of rotor blade would be impossible. The vibratory levels in helicopters can also be reduced by suitable structural modifications (Refs.6, 7) and/ or by employing structural optimisation techniques (Ref.8).

Hub or blade mounted passive pendulum type vibration absorbers (Refs.9, 10) have been successful in reducing the vibratory levels in helicopters. But their incorporation always leads to increase in rotor weight and aerodynamic drag. The other type of passive system is based on anti-resonant principle. Dynamic Anti-resonant Vibration Isolation(DAVI), Anti-Resonant Isolation System(ARIS) and Liquid Inertia Vibration Eliminator(LIVE) fall under this category (Refs.11-14). These isolation devices are usually mounted between the fuselage and the rotor or gearbox support system, as shown in Fig.1. They are tuned to provide a maximum vibration reduction at a specific frequency. Hence, for any change in the operating conditions, there will be a degradation in the performance of these devices.

Active control methodologies include Higher Harmonic Control (HHC) (Refs.15-

19), Individual Blade Control (IBC) (Ref.20), Active Flap Control (AFC) (Ref.21) and Active Control of Structural Response (ACSR) (Refs.22-27). It is important to note that HHC, IBC and AFC control schemes are provided in the rotating frame, while ACSR is employed in the nonrotating frame. Flight tests have shown that higher harmonic pitch control of the blade provides a substantial reduction of about $80\% - 90\%$ in the vibratory levels in the fuselage. However, this control scheme has many drawbacks, such as, (i) rotor blade stall at high speeds, (ii) high power requirements and (iii) difficulties in meeting the airworthiness criteria. Some of these drawbacks can be eliminated by using an Active Flap Control scheme of vibration reduction. Currently, research efforts are aimed at developing a smart actuator for Active Flap Control.

Recently, another vibration control scheme, based on a new concept of Active Control of Structural Response (ACSR) has been developed. The idea of ACSR scheme is based on the principle of superposition of two independent responses of a linear system such that the total response is zero. In the case of helicopters, the fuselage is excited by the application of controlled external actuators at selected locations such that the total response of the fuselage due to rotor loads and the external actuator forces is a minimum (Refs.22, 23). A schematic of the helicopter system with ACSR scheme is shown in Fig.1. The rotor loads ($F_{HX}, F_{HY}, F_{HZ}, M_{HX}, M_{HY}, M_{HZ}$) are transmitted to the fuselage through the gearbox support structure. The support structure is idealised as a spring, damper mechanism and a control force generator. In passive scheme, the control force generator corresponds to a vibration absorber mass (as in ARIS), whereas in the case of ACSR, the control force generator is an active electro-hydraulic force actuator. Preliminary studies based on extensive ground and flight tests have shown promising results in reducing vibration in helicopters.

The major advantages of ACSR scheme are: (i) less power requirements, (ii) minimal airworthiness requirements because this scheme is independent of the primary flight control systems, and (iii) selectively minimise vibratory levels at any set of chosen locations in the fuselage.

The first step in implementing any active vibration control scheme is the measurement of vibration. In general, the vibratory levels are measured at tail boom/tail rotor transmission, cockpit instrument mountings, cabin floor and pilot location (Refs.24-26). Even though, these locations may be sensitive, in the light of recent developments (Refs.28-30) on the optimal placement of sensors for system identification, an interesting question arises:*i.e., whether the measurement of vibration at the above mentioned locations truly represents the vibratory levels in the structure or not. In other words, whether the control of vibration at some selected sensitive points in the structure truly corresponds to a reduction of vibration in the whole structure or not.* A review on the sensor placement in distributed parameter(continuous) systems can be found in Ref.31. It is pointed out in Ref.30 that the measurement locations play a major role on the quality of measurement and in some situation modes may be completely missed. For a simple one dimensional structure, the measurement locations can be selected based on experience, but for complicated three dimensional structures the choice is very difficult. Therefore there is need for systematic approach based on mathematical principles to arrive at the optimal sensor locations. In Ref.28, Kammer has described a suboptimal procedure for identifying the sensor locations in large structures for the measurement of frequencies and mode shapes which can be compared with FEM results for correlation studies. This procedure is based on using Fisher Information Matrix and Effective Independence Distribution Vector (EIDV)

to eliminate sequentially the redundant sensor locations from an initial set of many candidate sensor locations. In Ref.29, this approach was slightly modified, by considering the controllability and observability matrices of the system, to identify the actuator/sensor placement in a truss structure for modal parameter (natural frequency and mode shape) identification. A comparative analysis of EIDV method and Guyan reduction approach is presented in Ref.30. The comparative study was based on identifying the sensor locations for modal testing of one-dimensional beams and two-dimensional plates. The application of EIDV approach for active control of vibrations in helicopters will be highly useful from the point of view of practical considerations and such a study has not been reported so far in the open literature.

Coupled rotor - fuselage vibration analysis has been studied by several researchers. Though, these studies provide significant contribution towards the understanding of the mechanism of helicopter vibration, most of the studies assume either a rigid fuselage or a 2-D beam type fuselage (Refs.14, 32-36). Since the frequencies of the complex helicopter structure with heavy concentrated masses will be closely placed (Ref.37), an analysis with simplified model of the structure cannot represent all the critical vibration modes of the fuselage. Hence, a meaningful study on analysis and control of vibration in helicopter requires a more realistic structural dynamic model of helicopter fuselage. Therefore, recent studies on vibration analysis use a 3-D model for the helicopter fuselage (Refs.27, 38). A three dimensional finite element model of a helicopter fuselage, shown in Fig.2, has been developed by Mangalick, *et. al* (Ref.39). The structural dynamic characteristics of this model resemble those of a realistic helicopter (Ref.39) and this model is used in the present study on vibration analysis and control.

1.1 Objectives

The main objectives of the present study are:

- Identification of optimal sensor locations for measurement of vibration in a 3-D finite element model of a helicopter fuselage for active control studies.
- Formulation of the equations of motion of a coupled gearbox-flexible fuselage helicopter system for vibration analysis.
- Formulation of an open-loop control scheme for vibration minimisation.
- Analyse the effectiveness of vibration control using the measurements from optimally placed sensors in comparison to the control of vibration using measurements from arbitrarily placed sensor locations.

Chapter 2

EQUATIONS OF MOTION FOR COUPLED ROTOR-GEARBOX-FLEXIBLE FUSELAGE SYSTEMS

The analytical study on helicopter vibration requires the development of the equations of motion representing the dynamics of the coupled rotor-gearbox-fuselage systems. The dynamic model must consist of

- Rotor blade model
- Gearbox model
- Fuselage model
- Rotor-Gearbox-Fuselage interface model

The rotor blade model requires the structural, inertial and aerodynamic operators associated with the rotor blade motion. The flexible helicopter fuselage can be idealised as a three dimensional finite element model. The rotor-gearbox-fuselage interface must represent the geometry of the interface as well as the aerodynamic interaction in an apporiate manner. A schematic of a helicopter system is shown in Fig.1. The main rotor system is attached to a rigid shaft from the gearbox. The gearbox is connected to the roof of the fuselage through a support structure.

2.1 Equations of Motion

A detailed description of the equations of motion of the coupled rotor-gearbox-fuselage system is provided below.

2.1.1 Blade Model

The rotor blade can be modelled as an elastic beam undergoing deformations in axial-flap-lag and torsional modes. The equations of motion of the blade in modal space can be written symbolically as

$$[M]_b\{\ddot{y}\} + [C]_b\{\dot{y}\} + [K]_b\{y\} + \{F\} = 0 \tag{2.1}$$

In this equation, the forcing function {F} contains all the non-linear terms, the aerodynamic loading and the effects due to translational and rotational rigid body motions of hub. The vector $\{y\}$ represents the generalised co-ordinates associated with the various blade modes. The blade loads contain all harmonics of the rotor rotational frequency. The

individual blade loads combine at the hub resulting in the concellation of some of the harmonics and the addition of those harmonics which are integer multiples of blade passage frequency. The hub loads in the non-rotating frame are obtained after summing up the loads associated with the individual blades in the rotating frame.

Let ${F^k}_{xR}, {F^k}_{yR}, {F^k}_{zR}$ and ${M^k}_{xR}, {M^k}_{yR}, {M^k}_{zR}$ represent the hub shears and hub moments due to the $k-th$ blade, in the rotating frame, respectively. (The hub-fixed non-rotating and the hub-fixed rotating co-ordinate systems are shown in Fig.3). The hub loads in the non-rotating frame can be written as

$$\begin{Bmatrix} F_{Hx} \\ F_{Hy} \\ F_{Hz} \end{Bmatrix} = \sum_{k=1}^{NB} \begin{bmatrix} \cos\psi_k & -\sin\psi_k & 0 \\ \sin\psi_k & \cos\psi_k & 0 \\ 0 & 0 & 1 \end{bmatrix} \begin{Bmatrix} {F^k}_{xR} \\ {F^k}_{yR} \\ {F^k}_{zR} \end{Bmatrix} \tag{2.2}$$

$$\begin{Bmatrix} M_{Hx} \\ M_{Hy} \\ M_{Hz} \end{Bmatrix} = \sum_{k=1}^{NB} \begin{bmatrix} \cos\psi_k & -\sin\psi_k & 0 \\ \sin\psi_k & \cos\psi_k & 0 \\ 0 & 0 & 1 \end{bmatrix} \begin{Bmatrix} {M^k}_{xR} \\ {M^k}_{yR} \\ {M^k}_{zR} \end{Bmatrix} \tag{2.3}$$

$$\psi_k = \psi_1 + 2\frac{\pi}{NB}(k-1) \qquad\qquad k = 1, \cdots NB$$

Where NB is the number of blades in the rotor system. The quantities F_{Hx}, F_{Hy}, F_{Hz} and M_{Hx}, M_{Hy}, M_{Hz} represent the hub shears and hub moments respectively.

2.1.2 Gearbox Equations

The gearbox is assumed to be rigid. The gearbox mounting have finite length and each one is idealised as a linear spring and a viscous damper element. In addition, a control force generating mechanism is acting prarallel to the spring and damper elements. A schematic of the mounting is shown in Fig.1.

The loads acting on the gearbox can be decomposed into two parts, one component consisting of the integrated rotor blade loads acting at the hub and the second part representing the load from the mountings. While the integrated rotor loads at the hub consist of forces and moments, the mountings are assumed to transfer only forces. The force applied by each mounting has three components, namely the damping force, the spring force and the control force. The gearbox support forces acting at point I, (Fig.1), can be expressed as

$$\begin{Bmatrix} F_{xi} \\ F_{yi} \\ F_{zi} \end{Bmatrix}_{GB} = -K_i \begin{bmatrix} l^2 & lm & ln \\ ml & m^2 & mn \\ nl & nm & n^2 \end{bmatrix} \left[\begin{Bmatrix} x_i \\ y_i \\ z_i \end{Bmatrix}_{GB} - \begin{Bmatrix} x_i \\ y_i \\ z_i \end{Bmatrix}_{F} \right]$$

$$-C_i \begin{bmatrix} l^2 & lm & ln \\ ml & m^2 & mn \\ nl & nm & n^2 \end{bmatrix} \left[\begin{Bmatrix} \dot{x}_i \\ \dot{y}_i \\ \dot{z}_i \end{Bmatrix}_{GB} - \begin{Bmatrix} \dot{x}_i \\ \dot{y}_i \\ \dot{z}_i \end{Bmatrix}_{F} \right] + \begin{Bmatrix} F_{xi} \\ F_{yi} \\ F_{zi} \end{Bmatrix}_{C} \quad (2.4)$$

$$i = 1, \cdots NC$$

The subscript i indicates the i-th mounting of the gearbox and NC is the total number of gearbox supports. l, m and n are direction cosines . of the i-th mounting

structure in equilibrium position. The vectors $\{x_i, y_i, z_i\}_{GB}$ and $\{x_i, y_i, z_i\}_F$ represent the displacements of the points I and I'. Points I and I' are the points of attachment of the i-th isolator to the gearbox and the fuselage respectively. K_i and C_i represent the stiffness and damping of the i-th gearbox mounting respectively. The control force vector $\{F_{xi}, F_{yi}, F_{zi}\}_C$ can be due to an active isolation device (ACSR) or due to a passive isolation device (ARIS).

The total force on the gearbox, consisting of forces due to isolators, rotor hub loads and gravity, can be written as

$$\left\{\begin{array}{c} F_x \\ F_y \\ F_z \end{array}\right\}_{GB} = \sum_{i=1}^{NC} \left\{\begin{array}{c} F_{xi} \\ F_{yi} \\ F_{zi} \end{array}\right\}_{GB} + \left\{\begin{array}{c} F_x \\ F_y \\ F_z \end{array}\right\}_{Hub} + \left\{\begin{array}{c} F_x \\ F_y \\ F_z \end{array}\right\}_{Gravity} \tag{2.5}$$

The total moment about the centre of mass of the gearbox is given as

$$\left\{\begin{array}{c} M_x \\ M_y \\ M_z \end{array}\right\}_{GB} = \sum_{i=1}^{NC} \left\{\begin{array}{c} p_{yi}F_{zi} - p_{zi}F_{yi} \\ p_{zi}F_{xi} - p_{xi}F_{zi} \\ p_{xi}F_{yi} - p_{yi}F_{xi} \end{array}\right\}_{GB} + \left\{\begin{array}{c} H_yF_z - H_zF_y \\ H_zF_x - H_xF_z \\ H_xF_y - H_yF_x \end{array}\right\}_{Hub} + \left\{\begin{array}{c} M_x \\ M_y \\ M_z \end{array}\right\}_{Hub} \tag{2.6}$$

The rigid body perturbational equations of motion of gearbox are obtained after subtracting the mean values of the forces and moments from the total loads. These equations can be written as,

Perturbational Translation Equations

$$\left\{\begin{array}{c} F_x - F_{xm} \\ F_y - F_{ym} \\ F_z - F_{zm} \end{array}\right\}_{GB} = \left[\begin{array}{ccc} m & 0 & 0 \\ 0 & m & 0 \\ 0 & 0 & m \end{array}\right]_{GB} \left\{\begin{array}{c} \ddot{x}_{GB} \\ \ddot{y}_{GB} \\ \ddot{z}_{GB} \end{array}\right\} \tag{2.7}$$

Perturbational Rotation Equations

$$\{\tilde{M} - \tilde{M}_m\}_{GB} = \dot{\vec{H}}_{GB} + \vec{\omega} \times \vec{H}_{GB} \tag{2.8}$$

where,

$$\vec{H}_{GB} = \begin{Bmatrix} H_x \\ H_y \\ H_z \end{Bmatrix}_{GB} = \begin{bmatrix} I_{xx} & I_{xy} & I_{xz} \\ I_{yx} & I_{yy} & I_{yz} \\ I_{zx} & I_{zy} & I_{zz} \end{bmatrix}_{GB} \begin{Bmatrix} \dot{\theta}_{xGB} \\ \dot{\theta}_{yGB} \\ \dot{\theta}_{zGB} \end{Bmatrix}$$

$$\vec{\omega} = \dot{\theta}_{xGB}\ \hat{i} + \dot{\theta}_{yGB}\ \hat{j} + \dot{\theta}_{zGB}\ \hat{k}$$

2.1.3 Fuselage Equations

The fuselage is idealised as a three dimensional finite element model, shown in Fig.2. The finite elements considered are simple one dimensional beam elements with uniform properties. Rotary inertia and shear deformation have been neglected. Lumped masses representing equipment, engines, fuel, tail gearbox and end plates are attached to the structure at appropriate node locations. The forces acting on the fuselage are those acting at the gearbox mountings, tail rotor loads, gravity and fuselage aerodynamic loads.

The total force on the helicopter fuselage can be expressed as

$$\begin{Bmatrix} F_x \\ F_y \\ F_z \end{Bmatrix}_F = \sum_{i=1}^{NC} - \begin{Bmatrix} F_{xi} \\ F_{yi} \\ F_{zi} \end{Bmatrix}_{GB} + \begin{Bmatrix} F_x \\ F_y \\ F_z \end{Bmatrix}_{Aerodynamic} + \begin{Bmatrix} F_x \\ F_y \\ F_z \end{Bmatrix}_{Gravity} + \begin{Bmatrix} F_x \\ F_y \\ F_z \end{Bmatrix}_{Tail} \tag{2.9}$$

The moment about the centre of gravity of the fuselage can be written as

$$\left\{\begin{array}{c} M_x \\ M_y \\ M_z \end{array}\right\}_F = \sum_{i=1}^{NC} - \left\{\begin{array}{c} h_{yi}F_{zi} - h_{zi}F_{yi} \\ h_{zi}F_{xi} - h_{xi}F_{zi} \\ h_{xi}F_{yi} - h_{yi}F_{xi} \end{array}\right\}_F + \left\{\begin{array}{c} h_{yT}F_z - h_{zT}F_y \\ h_{zT}F_x - h_{xT}F_z \\ h_{xT}F_y - h_{yT}F_x \end{array}\right\}_{Tail}$$

$$+ \left\{\begin{array}{c} M_x \\ M_y \\ M_z \end{array}\right\}_{Aerodynamic} + \left\{\begin{array}{c} M_x \\ M_y \\ M_z \end{array}\right\}_{Tail} \tag{2.10}$$

For equilibrium condition, the mean values of the gearbox support forces and moments acting on the fuselage must balance the steady components of the fuselage aerodynamic, gravity and tail rotor loads. In this formulation, it is assumed that the fuselage aerodynamic loads and tail rotor loads are constants. The equations of motion of the fuselage are as follows

Perturbational Translation Equations

$$\left\{\begin{array}{c} F_x - F_{xm} \\ F_y - F_{ym} \\ F_z - F_{zm} \end{array}\right\}_F = \left[\begin{array}{ccc} m & 0 & 0 \\ 0 & m & 0 \\ 0 & 0 & m \end{array}\right]_F \left\{\begin{array}{c} \ddot{x}_F \\ \ddot{y}_F \\ \ddot{z}_F \end{array}\right\} \tag{2.11}$$

Perturbational Rotation Equations

$$\{\tilde{M} - \tilde{M}_m\}_F = \dot{\vec{H}}_F + \vec{\omega} \times \vec{H}_F$$

where,

$$\vec{H}_F = \left\{ \begin{array}{c} H_x \\ H_y \\ H_z \end{array} \right\}_F = \left[\begin{array}{ccc} I_{xx} & I_{xy} & I_{xz} \\ I_{yx} & I_{yy} & I_{yz} \\ I_{zx} & I_{zy} & I_{zz} \end{array} \right]_F \left\{ \begin{array}{c} \dot{\theta}_{xF} \\ \dot{\theta}_{yF} \\ \dot{\theta}_{zF} \end{array} \right\} \tag{2.12}$$

$$\vec{\omega} = \dot{\theta}_{xF}\ \hat{i} + \dot{\theta}_{yF}\ \hat{j} + \dot{\theta}_{zF}\ \hat{k} \tag{2.13}$$

Fuselage Elastic Mode Equations

The vibratory loads acting on the fuselage are only due to the main rotor. These loads are transmitted to the fuselage at the gearbox support points. The fuselage flexible mode equations in modal space can be written as,

$$[\bar{M}]\{\ddot{\eta}\} + [\bar{C}]\{\dot{\eta}\} + [\bar{K}]\{\eta\} = \{Q_F\} \tag{2.14}$$

where,

$\{\eta\}$ represents the modal vector,

and ${Q^j}_F$ is the generalised force for the j-th vibrational mode, which is given as,

$$Q^j_F = \sum_{i=1}^{NC} -\{(F_x - F_{xm})\ (F_y - F_{ym})\ (F_z - F_{zm})\}^i_{GB} \left\{ \begin{array}{c} {\Psi^i}_{jx} \\ {\Psi^i}_{jy} \\ {\Psi^i}_{jz} \end{array} \right\} \tag{2.15}$$

Chapter 3

REDUCED SET OF EQUATIONS FOR VIBRATION AND CONTROL ANALYSES

The coupled set of equations of motion for the rotor-gearbox-fuselage dynamics, formulated in Chapter 2, are simplified for the purpose of the present study on active vibration control in helicopters. In these simplified models, the rotor blade dynamics are not included. However, the hub loads due to the rotor blades are assumed to be acting at the top of the gearbox, as shown Fig.4. Several assumptions have been made in formulating the simplified set of equations.

3.1 Assumptions

1. The gearbox is assumed to be rigid and undergoes vertical translation (z_{GB}), pitch (θ_{yGB}) and roll (θ_{xGB}) motions.

2. The fuselage is assumed to be undergoing rigid body vertical translation (z_F), pitch (θ_{yF}) and roll (θ_{xF}) motions, as well as flexible deformation due to elastic modes.

3. Only the vertical component, $F_z(t)$, of the hub loads is assumed to be acting at the top of the gearbox, simulating a ground test condition.

4. The gearbox supports are assumed to be uni-axial members providing forces, only in the z-direction.

5. The centre of mass of the gearbox is assumed to be above the centre of mass of fuselage on same vertical axis.

6. The rigid body rotational motions of the gearbox and fuselage are assumed to be small. Hence, the nonlinear terms involving products of rotational degrees of freedom have been neglected.

7. The products of inertia of the gearbox and the fuselage are assumed to be zero.

3.2 Equations of Motion of Coupled Gearbox-Fuselage System

The equations of motion of the coupled gearbox-fuselage system can be written in three sets. Set I describes the rigid body equations of motion of the gearbox; Set II presents the rigid body equations of motion of the fuselage and Set III represents the equations of motion of the elastic modes of the fuselage. The details of the derivation are given below.

3.2.1 Set I: Gearbox Rigid Body Translational and Rotational Equations

The force F_i due to the spring and damper (Fig.1), acting at the i-th gearbox support can be expressed as,

$$F_i = K_i(z_{GB} - \theta_{yGB}\, p_{xi} + \theta_{xGB}\, p_{yi} - z_i) + C_i(\dot{z}_{GB} - \dot{\theta}_{yGB}\, p_{xi} + \dot{\theta}_{xGB}\, p_{yi} - \dot{z}_i) \quad (3.1)$$

where z_i and $\dot{z}_i$ represent the total displacement and total velocity at i-th gearbox support point in the fuselage respectively. These can be written as

$$z_i = z_F - \theta_{yF}\, h_{xi} + \theta_{xF}\, h_{yi} + \sum_{j=1}^{Nm} \Psi^i{}_{jz}\eta_j(t) \quad (3.2)$$

$$\dot{z}_i = \dot{z}_F - \dot{\theta}_{yF}\, h_{xi} + \dot{\theta}_{xF}\, h_{yi} + \sum_{j=1}^{Nm} \Psi^i{}_{jz}\,\dot{\eta}_j(t) \quad (3.3)$$

Translational Equation

$$m_{GB}\,\ddot{z}_{GB} = F_z(t) - \sum_{i=1}^{NC}(F_i - F_c{}^i) \quad (3.4)$$

$F_c{}^i$ represents the control force at the i-th gearbox support.

Rotational Equations

$$\text{Pitch Equation} \qquad I_{yyGB}\,\ddot{\theta}_{yGB} = \sum_{i=1}^{NC}(F_i\, p_{xi} - F_c{}^i\, p_{xi}) \quad (3.5)$$

$$\text{Roll Equation} \qquad I_{xxGB}\,\ddot{\theta}_{xGB} = -\sum_{i=1}^{NC}(F_i\, p_{yi} - F_c{}^i\, p_{yi}) \quad (3.6)$$

3.2.2 Set II: Fuselage Rigid Body Translational and Rotational Equations

Translational Equation

$$m_F \ddot{z}_F = \sum_{i=1}^{NC}(F_i - F_c^i) \tag{3.7}$$

Rotational Equations

Pitch Equation
$$I_{yyF} \ddot{\theta}_{yF} = -\sum_{i=1}^{NC}(F_i\, h_{xi} - F_c^i\, h_{xi}) \tag{3.8}$$

Roll Equation
$$I_{xxF} \ddot{\theta}_{xF} = \sum_{i=1}^{NC}(F_i\, h_{yi} - F_c^i\, h_{yi}) \tag{3.9}$$

3.2.3 Set III: Fuselage Elastic Mode Equations

The equations of motion of the elastic modes of the fuselage can be written symbollically as,

$$[\bar{M}]\{\ddot{\eta}\} + [\bar{C}]\{\dot{\eta}\} + [\bar{K}]\{\eta\} = \{Q_F\} \tag{3.10}$$

The generalised force in the j-th mode, ${Q^j}_F$ can be written as

$${Q^j}_F = \sum_{i=1}^{NC} F_i\, {\Psi^i}_{jz} - \sum_{i=1}^{NC} {F^i}_c\, {\Psi^i}_{jz} \qquad j = 1, 2.....Nm \tag{3.11}$$

Where Nm is the number of elastic modes of the fuselage considered for vibration analysis.

Equations (3.4-3.10) constitute the complete set of linear, coupled differential equations used for the vibration analysis. These equations are nondimensionalised using radius (R) of the blade for length units, mass of blade (m_B) for mass units and rotor speed of

rotation (Ω) for time. For mathematical convenience, the nondimensional equations are written in state space form as

$$\left\{ \dot{q} \right\} = [\, A \,]\{q\} + [\, B \,]\{U\} + \{f\} \tag{3.12}$$

where,

$$\left\{ q \right\} = \begin{Bmatrix} q_1 \\ q_2 \end{Bmatrix}$$

$$\left\{ q_1 \right\} = \begin{Bmatrix} z_{GB} \\ \theta_{yGB} \\ \theta_{xGB} \\ \cdots \\ z_F \\ \theta_{yF} \\ \theta_{xF} \\ \cdots \\ \eta_1 \\ \eta_2 \\ \vdots \\ \eta_{Nm} \end{Bmatrix}_{(6+Nm)\times 1} \qquad \text{and} \qquad \left\{ q_2 \right\} = \left\{ \dot{q}_1 \right\}$$

$$\left\{ f \right\} = \left\{ \begin{array}{l} \{0\}_{(6+Nm)\times 1} \\ \cdots \\ \frac{F_z(t)}{m_{GB}} \\ 0 \\ 0 \\ \vdots \\ 0 \end{array} \right\}_{2(6+Nm)\times 1}$$

$$\left\{ U \right\} = \left\{ \begin{array}{l} F^1{}_c \\ F^2{}_c \\ \vdots \\ F^i{}_c \end{array} \right\}_{NC\times 1}$$

The details of system matrices [A] and [B] are given in Appendix A. It may be noted that the nondimensional quantities are represented by same symbols as the dimensional quantities in Eq.(3.12) as well as in the following sections, for convenience.

Chapter 4

SELECTION OF SENSOR LOCATIONS FOR VIBRATION MEASUREMENT

The first step in implementing any active vibration control scheme is the measurement of vibration. The sensors must be placed at appropriate locations which do not coincide with the nodal points of the vibratory modes. For complex three dimensional structure, the selection of sensor locations is a difficult task. In practice, optimal sensor locations for vibration measurement are identified by performing extensive shake tests, Refs.(23, 24). Therefore, there is strong need for a systematic approach based on mathematical principles to arrive at the optimal sensor locations for vibration measurement and control. In recent publications, Refs.(28-31), a sub-optimal procedure has been developed for identifying the sensor locations in large space structures for the measurement of frequencies and mode shapes. This procedure is based on using *Fisher Information Matrix* and *Effective*

Independence Distribution Vector (EIDV) to eliminate sequentially the redundant sensor locations from an initial set of many candidate sensor locations. The application of EIDV approach for active control of vibration in helicopters will be highly useful from practical considerations.

This Chapter describes the EIDV approach to arrive at the appropriate sensor locations for vibration measurement and control.

4.1 Mathematical Model

The equations of motion of a flexible structure in finite element domain can be written as

$$[M]_F\{\ddot{x}\} + [C]_F\{\dot{x}\} + [K]_F\{x\} = \{F\} \tag{4.1}$$

where $[M]_F, [C]_F, [K]_F$ and {F} represent the mass, damping, stiffness matrices (of dimension N×N) and the external force vector(of size N×1) respectively. Considering the first Nm undamped modes, the modal transformation relation can be written as

$$\{x\} = [\Phi]\{\eta\} \tag{4.2}$$

Substituting Eq.(4.2) in Eq.(4.1) and premultiplying by $[\Phi]^T$ yeilds

$$[\bar{M}]\{\ddot{\eta}\} + [\bar{C}]\{\dot{\eta}\} + [\bar{K}]\{\eta\} = \{Q_F\} \tag{4.3}$$

where $[\bar{M}], [\bar{C}], [\bar{K}]$ have a dimension of $Nm \times Nm$ and $\{\eta\}$, $\{Q_F\}$ are vectors of size $Nm \times 1$.

Assuming harmonic input excitation $\{\mathrm{F}\} = \{\bar{F}\}e^{i\omega t}$ where ω is a constant, the steady state displacement at any point on the structure can be expressed as

$$\{y\} = [\Phi_s]\{\eta\} \tag{4.4}$$

where the dimension of $\{y\}$ is $M_L \times 1$ and M_L represents the initial number of candidate sensor locations. Φ_s represents the modal matrix corresponding to the initial set of candidate sensor locations.

To start with, it is assumed that the initial number of candidate sensor locations is greater than the number of modal co-ordinates (*i.e.*,$M_L > Nm$). In state feed back control, an estimate of the states of the system is required and the best estimate can be obtained from the following equations.

$$\{\hat{\eta}\} = \underbrace{[\Phi_s{}^T\Phi_s]^{-1}\Phi_s{}^T}\{y\} \tag{4.5}$$

The underbraced term in Eq.(4.5) is denoted as Moore-Penrose inverse or pseudo-inverse (Ref.40) of Φ_s. Since the dimension of Φ_s is $(M_L \times Nm)$ and $M_L > Nm$, the rank of Φ_s is equal to Nm which is same as the number of modal co-ordinates. Hence, there are $(M_L$ - $Nm)$ rows in Φ_s which are linearly dependent on the remaining Nm rows. Physically, it means that there are $(M_L$ - $Nm)$ additional sensors providing redundant information about the Nm modal co-ordinates. From the point of view of reachability of certain locations and also due to the cost of sensors, it is not possible to have sensors at all locations. Generally, the number of available sensors (M_A) is less than the number of initial candidate measurement locations and it can be greater than or equal to the number of modes (*i.e.*, $Nm \leq M_A < M_L$). The aim is to eliminate those sensors which provide redundant information about the system response. In Eq.(4.5), the symmetric matrix $[\Phi_s{}^T\Phi_s]$ is denoted as *Fisher Information Matrix.* Premultiplying Eq.(4.5) by Φ_s yields

$$\Phi_s\{\hat{\eta}\} = \underbrace{\Phi_s[\Phi_s{}^T\Phi_s]^{-1}\Phi_s{}^T}\{y\} = \{\hat{y}\} \tag{4.6}$$

If Φ_s is a non-singular square matrix, then the underbraced term in Eq.(4.6) will be a unit matrix. For a general case, let the underbraced term in Eq.(4.6) be denoted by the symbol E.

$$E = \Phi_s[\Phi_s{}^T\Phi_s]^{-1}\Phi_s{}^T \tag{4.7}$$

Matrix E is an *idempotent* matrix *i.e.*, $E = E^2$ and its eigenvalues are either 0 or 1. In addition, the trace of the *idempotent* matrix E is equal to its rank (Ref.40). Hence, the diagonal elements of E represent the fractional contribution to the rank of E and the smallest diagonal element (say, E_{ii}) contributes the least to the rank of E. Since the rank of E is equal to the rank of Φ_s, the i-th row of Φ_s contributes the least to the rank of Φ_s. Therfore, the i-th row of Φ_s can be eliminated without influencing its rank. After eliminating the i-th row, the modified Φ_s having a reduced size is used to compute the new E matrix and the process of elimination is repeated. This procedure is carried out sequentially until the number of rows of Φ_s is equal to the number of available sensors M_A. The vector formed by the diagonal elements of E is denoted as the *Effective Independence Distribution Vector* (EIDV).

Since the inverse of *Fisher Information Matrix* is required to estimate the modal vector, (Eq.4.5), it is important to monitor its **Condition Number** at every iteration. If there is a drastic increase in the condition number, then the elimination process has to be terminated. It may be noted that the condition number of a square matrix represents the sensitivity of its inverse to very small changes in the elements of the matrix (Ref.41). The definition of condition number is provided in Appendix B.

In every iteration, one can eliminate either one row (one sensor) or a group of

rows (group of sensors) whose corresponding diagonal elements (E_{ii}) are very small in comparison to other diagonal elements (as carried out in Refs.28, 29). In identifying the optimal sensor locations, the advantage of group elimination is that it requires less number of iterations as compared to single elimination. However, the disadvantage will be that there is a likelihood of increasing the condition number of the Fisher Information Matrix. This important conclusion is brought out in Chapter 6, while presenting the results of a comparative analysis of single elimination and group elimination.

Chapter 5

VIBRATION CONTROL

During steady forward flight, the helicopter experiences periodic hub loads. The predominant frequency of the hub loads is NB/rev, where NB is the number of blades in the rotor system. These vibratory loads excite the fuselage structure. The vibratory levels in the fuselage are measured by a set of optimally placed sensors. Using the measurements from the sensors, an open-loop (Multi-Input-Multi-Output) control scheme is formulated to minimise the vibration in the fuselage.

5.1 Open-Loop Control Formulation For Vibration Reduction

The equations of motion of the coupled gearbox-fuselage model have been derived in Chapter 3. These equations can be written in state space form as (Eq.3.12)

$$\{\dot{q}\} = [A]\{q\} + [B]\{U\} + \{f\} \tag{5.1}$$

The sensors measure vibratory response of the fuselage. The sensor measurements can be written as

$$\{Y\} = [C]\{q\} \tag{5.2}$$

The details of $[A]$, $[B]$, $[C]$, $\{q\}$ and $\{f\}$ are given in Chapter 3 and in Appendix A. For harmonic input $\{f\} = \{\bar{f}\}e^{i\omega t}$, the steady state response can be written as,

$$\{q\} = [A - i\omega I]^{-1}[B]\{U\} + [A - i\omega I]^{-1}\{f\} \tag{5.3}$$

The vibratory response measured at preselected sensor locations can be written as

$$\begin{aligned} \{Y_s\} &= [C]_s\{q\} \\ &= [C]_s[A - i\omega I]^{-1}[[B]\{U\} + \{f\}] \\ &= [T]\{U\} + \{b\} \end{aligned} \tag{5.4}$$

where,

$$\begin{aligned} [T] &= [C]_s[A - i\omega I]^{-1}[B] \\ \{b\} &= [C]_s[A - i\omega I]^{-1}\{f\} \end{aligned}$$

Formulating a minimization problem as

$$min \;\; J = \{Y\}^T{}_s \, \{Y\}_s \qquad \text{w.r.t} \;\; \{U\} \tag{5.5}$$

Substituting for $\{Y\}_s$ from Eq.(5.4) yields

$$min \;\; J = U^T T^T T U + b^T T U + U^T T^T b + b^T b \tag{5.6}$$

Differentiating J with respect to $\{U\}$ yields

$$\frac{\partial J}{\partial \{U\}} = 2T^T T U + 2T^T b = 0 \tag{5.7}$$

From Eq.(5.7), the best estimate of the control vector minimizing the performance index can be written as

$$\hat{U} = -[T^T T]^{-1} T^T b \tag{5.8}$$

Substituting $\{\hat{U}\}$ from Eq.(5.8) and using Eq.(5.2), the controlled vibratory response at any location in the coupled gearbox-fuselage system can be obtained. It is important to note the control force vector $\{\hat{U}\}$ is estimated using the vibratory response at only certain preselected locations in the system. For example, these preselected locations could be the optimally identified locations or they could represent any set of arbitrarylocations.

Chapter 6

RESULTS AND DISCUSSION

Using the dynamic model of the coupled gearbox-flexible fuselage system, several studies were performed. The results of these studies are presented in three sections. First section describes the results pertaining to the study on the choice of sensor locations for vibration measurement. The second section presents the results of a vibration analysis of the coupled gearbox-fuselage model. The results of the study on vibration control in fuselage are presented in the third section.

6.1 Choice of Sensor Locations for Vibration Measurement

Using the mathematical formulation presented in Chapter 4 on EIDV approach, optimal sensor locations have been identified in a three dimensional finite element model of a helicopter fuselage. Before presenting the results corresponding to the helicopter fuselage problem, an example problem has been solved to highlight the essential features of the EIDV approach.

6.1.1 Example Problem

Consider an example in which there are six candidate measurement locations and $(y_i, i = 1, \cdots, 6)$ and three modes represented by the generalised co-ordinates (η_1, η_2, η_3), which is given as

$$\{y\} = [\Phi_s]\{\eta\} \tag{6.1}$$

where,

$$\left\{ y \right\} = \begin{Bmatrix} y_1 \\ y_2 \\ y_3 \\ y_4 \\ y_5 \\ y_6 \end{Bmatrix}$$

$$\left[\Phi_s \right] = \begin{bmatrix} 1 & 0 & 0 \\ 0 & 1 & 0 \\ 0 & 0 & 1 \\ 2 & 0 & 0 \\ 3 & 0 & 0 \\ 4 & 2 & 0 \end{bmatrix}$$

$$\left\{ q \right\} = \begin{Bmatrix} \eta_1 \\ \eta_2 \\ \eta_3 \end{Bmatrix}$$

The three column vectors of Φ_s correspond to the modal displacements at the six measurement locations. In this example, the rank of Φ_s is 3. The 4-th and 5-th rows of Φ_s are integer multiples of 1-st row. The 6-th row is a linear combination of rows 1 and 2. A sensor placed at location 6 will measure a maximum displacement in mode 1 and mode 2. A sensor at location 3 is essential to measure the 3-rd mode. In this case, a minimum of three sensors are required to estimate the three generalised co-ordinates. It is essential to have one sensor at location 3, preferable to have the second sensor at locations 6 and the third sensor can be placed at anyone of the remaining four (1,2,4 and 5) locations. Using the EIDV approach, the redundant sensor locations are eliminated sequentially one at a time. The results of the sequential elimination are provided in Table 1.

Table 1 contains $[\Phi_s]_j$ and $[E]_j$ (subscript j refers to j-th iteration) at every iteration along with the lowest diagonal value of $[E]_j$. In the first iteration, the lowest diagonal value of E is E_{11} which is $\frac{5}{86}$. Therefore the first row has the least influence on the rank of Φ_s. Eliminating the first row (i.e., the sensor at location 1), the new $[\Phi_s]_2$ is formed for the second iteration. In the second iteration, the lowest diagonal value of $[E]_2$ is E_{33} which is $\frac{20}{81}$. Eliminating this row (note that this row corresponds to the sensor location 4 in the original set of six sensor locations), the new $[\Phi_s]_3$ for the third iteration is formed. In the third iteration, the lowest diagonal value of $[E]_3$ is E_{11} which is $\frac{25}{61}$. Eliminating this row (i.e., the sensor at location 2 in the original set of six locations), the final $[\Phi_s]_4$ is formed. In this case, $[E]_4$ is an identity matrix, indicating that all diagonal elements (i.e., all sensors) are equally important. Further elimination of any one row will render the Fisher Information Matrix a singular matrix. This means that we are attempting to estimate three generalised (independent) co-ordinates with two sensor measurements, which is not possibe. In this example, the condition number of the Fisher Information Matrix exhibits a very small variation with iteration.

The final set of optimal locations for the sensors are at locations 3, 5, and 6. It is interesting to note that in all iterations, the value of the diagonal element corresponding to the sensor at location 3 is always one, indicating that this sensor is very important as noted earlier. The trace of the matrix E in every iteration is equal to 3, which is the rank of Φ_s. Another important observation is that the diagonal elements of E cannot be greater than 1. A formal mathematical proof for this statement can be found in Ref.28.

6.1.2 Helicopter Fuselage Problem

Figure 2 shows the baseline finite element model of a helicopter fuselage. The length of the helicopter model is 8.25m, the height is 2m, and the width is 3m. The fuselage is 4m long, having a width of 2.5m and a height of 1.5m. The tail boom is 4.25m in length, with a horizontal stabilizer having a span of 3m attached near the end. The total structural mass is 418.6kg. In addition, lumped masses representing two engines (each weighing 180kg), tail gearbox (weighing 40kg) and two end plates (each weighing 2kg) are also attached to structure at appropriate nodes. For the basleine configuration, the weight of one engine is uniformly distributed at nodes 41, 45 and 46; the other engine weight is unformly distributed at nodes 44, 48 and 49. The tail gearbox is placed at node 64. The weight of end plates are lumped at nodes 56 and 62 of the horizontal stabilizer. Total number of nodes and the degrees of freedom of the finite element model are 64 and 384 respectively. The details of the structural properties, node locations and other data are given in Ref.39. It was shown in Ref.39 that the undamped natural frequencies and mode shapes of this model are similar to those of a realistic helicopter. This model is used in the present study on the selection of sensor locations and vibration control. Figure 5 shows the first four modes of the fuselage. Table 2 presents the natural frequencies of the first 20 modes of the baseline configuration of the helicopter along with the nondimensional values.

Assuming that the main rotor system consists of four blades, the vibratory hub loads will have a nondimensional excitation frequency of 4/rev. It is evident from Table 2 that, the frequency of the rotor excitation loads is well below the natural frequency of the 20-th mode which is 6.4064. Therefore, it is more than sufficient to consider the first 20 modes for the vibration analysis of the helicopter fuselage. (The validity of this statement is proved by performing a convergence study on the vibration analysis, the results of which will be presented in Section 6.2).

Considering the first 20 modes of the fuselage (Nm=20), the modal matrix Φ_s is formulated. Since the vibratory level in the vertical (z) direction is more predominant, without loss of generality, it is assumed that the sensors measure only the z-component of the fuselage vibration. Therefore, in the formulation of Φ_s, the modal displacement in the z-direction only is considered. Initially it is assumed that all the 64 nodes are the candidate sensor locations (i.e., M_L= 64). The redundant sensor locations were eliminated by single elimination (one at each iteration) or by group elimination.

The results corresponding to single elimination procedure are shown in Figs.6 and 7. The variation of condition number of the Fisher Information Matrix with iteration number is shown in Fig.6. In this figure, the quantities within the bracket represent the number of sensors and the arrows indicate the value of condition number at the corresponding iteration. In the first iteration, there are 64 sensors and the condition number for this case is 2.86E+05. It is observed that the condition number remains more or less same till 39-th iteration. Then in the next 6 iterations, the condition number increases from around 3.55E+05 to 7.22E+05, but the order remains the same. At the end of 44-th iteration, there are 20 sensors and the corresponding condition number is 7.22E+05. These optimally selected 20 sensor locations are shown by node numbers in Fig.7.

The result of group elimination is shown in Fig.8. In this case, in every iteration, group of sensors, whose corresponding E_{ii} values in Effective Independent Distribution Vector (EIDV) are almost equal, are eliminated. The variation of condition number with iteration is shown in Fig.8. In the first iteration, there are 64 sensors and the corresponding condition number is 2.86E+05. Till 13-th iteration, the condition number remains more or less in the same order. There are 25 sensors in the 13-th iteration and the corresponding condition number is 9.02E+05. With further elimination of sensors, the condition number increases drastically. In the 14-th iteration, there are 23 sensors with a condition number equal to 1.69E+13. Since there is a drastic increase in the condition number, the elimination process is terminated at the 14-th iteration.

Comparing the results shown in Figs.6 and 8, it is interesting to note that even with 23 sensors, identified by the group elimination process, the condition number is of the order of 1.0E+13, whereas with 20 sensors, identified by the single elimination process, the condition number is of the order of 1.0E+05.

6.1.3 Failure Analysis of Sensors

A preliminary study is carried out to analyse the effect of sensor failure on the quality of state estimation. The parameter used for comparing the quality of estimation is the condition number of the Fisher Information matrix. It is assumed that initially a redundant set of 25 sensors are available for the estimation of response of 20 modes. Two sets of 25 sensors were chosen; one set is obtained by group elimination and the other set by single

elimination.

The study of failure analysis is carried out for two cases. In the first case, any one sensor is assumed to fail at a given instant. It may be noted that there 25 combinations of failure for 25 sensors. In the second case, it is assumed that any two sensors can fail at a given instant; for this case there are 300 combinations of failure for 25 sensors. For all these combinations of failure, the condition number of Fisher Information matrix is calculated after eliminating the row, corresponding to the failed sensor, from the matrix Φ_s. Then, the condition numbers corresponding to the various combinations of failure are arranged in ascending order. Figure 9 shows the variation of condition number for one sensor failure analysis and Fig.10 shows the variation for two sensors failure analysis. The arrows in the figures indicate the range of variation of condition number. It can be seen from Fig.9 that the range of variation of condition number, for sensors obtained by single elimination, is very small compared to that for the sensor set obtained by group elimination. A similar observation can also be seen in Fig.10, for two sensors failure analysis. In this case(Fig.10), the range of variation of condition number for group elimination case is of the order of 1.0E+08, while the range of variation for the single elimination case, is of the order 1.0E+01. These results clearly indicate that single elimination approach of selecting the optimal sensor locations provides a very stable condition number for Fisher Informatiom matrix than the group elimination process.

6.1.4 Condition Number and Normalisation of Modal matrix

It can be seen from the results that even for single elimination, the absolute value of the condition number (order of 1.0E+05) of Fisher Information matrix is quite high. However, in the selection of sensor locations, the variation in the order of condition number is more important than the absolute value itself. The reason is that the condtion number of the modal matrix can be arbitrarily varied by employing different normalisation factors for different modal vectors. This point is illustrated in the following example.

Consider a matrix Φ_s, whose size is 3×2. The two modes correspond to the first two modes of uniform cantilever beam. A modified matrix $\bar{\Phi}_s$ is obtained by multiplying

two columns of Φ_s by different multiplication factors.

$$\left[\ \Phi_s\ \right] = \begin{bmatrix} 0 & 0 \\ 0.2776 & -0.5287 \\ 1.00 & 1.00 \end{bmatrix}$$

$$\left[\ \bar{\Phi}_s\ \right] = \begin{bmatrix} 0 & 0 \\ 0.02776 & -0.005287 \\ 0.1 & 0.01 \end{bmatrix}$$

The condition number of the Fisher Information matrix $[{\Phi_s}^T \Phi_s]$ is 7, whereas the condition number of $[{\bar{\Phi}_s}^T \bar{\Phi}_s]$ is 207. It is interesting to note that the condition number of modal matrix can be arbitrarily changed by suitable multiplication factors.

6.1.5 Sensitivity of Sensor Locations to Modifications in Fuselage Structure

A study was conducted to analyse the sensitivity of sensor locations to modifications in the finite element model of helicopter fuselage structure. From the baseline configuration, the fuselage structure was modified by shifting the weight of one engine from node 48 to node 49. All the other data remain same. The natural frequencies and mode shapes of the modified structure were calculated. Table 3 presents the natural frequencies of the modified structure along with those of the baseline configuration. From this Table, it can be seen that there is very little change in the natural frequencies of the structure due to the modification. Using the modified structure, optimal locations for 20 sensors were obtained by single elimination approach and these locations are shown in Fig.11. Comparing Figs.7 and 11, it is noted that from the baseline case, the sensor at node 12 is moved to node 8; sensor at node 20 is shifted to node 27 and sensor at node 43 is shifted to node 39.

This study indicates that the EIDV approach for the selection of optimal sensor locations seems to be rather reasonably sensitive to structural modifications.

6.1.6 Validation of Optimal Sensor Locations

A vibration analysis was performed using the coupled gearbox-fuselage equations, by applying a vibratory force at the top of the gearbox. Total number of degrees of freedom considered in this analysis are 26. These include 3 rigid body modes of the gearbox (heave, pitch and roll), 3 rigid body modes and 20 flexible modes of the fuselage. The data used for the vibrational analysis are given in Table 4.

The vibratory levels in the fuselage were calculated for different excitation frequency, namely, 1/rev, 2/rev, 3/rev, 4/rev and 5/rev. The results of this analysis are shown in Figs.12-16. In these figures, the vibratory levels (g-levels) at different nodes are indicated by impulses. The arrows indicate the optimal locations for the sensors obtained by single elimination process. It is interesting to note from these figures that irrespective of the input excitation frequency, the optimally placed sensors measure high levels of vibration. For 1/rev excitation, the sensor at node 64 measures the highest level of vibration of 0.48g (Fig.12). For 2/rev excitation, though there is no sensor at node 38, where the g-level is maximum, there is a sensor at node 37 measuring the second highest level of vibration of 0.65g (Fig.13). For 3/rev excitation, the peak response is at node 38. But there is a sensor at node 37 measuring the second highest level of vibratory response (Fig.14). For 4/rev (Fig.15) and 5/rev (Fig.16) excitations, the peak response occurs at node 33. But there are two sensors at node locations 32 and 34 measuring the second highest level of response. These results indicate that the optimally selected sensors measure high levels of vibration.

6.2 Vibration Analysis

Assuming that the rotor system consists of four blades, a 4/rev hub vibratory load is applied at the top of the gearbox. Since the vertical load is predominant, for the purpose of analysis, only vertical component of load ($F_z(t)$) is applied. The gearbox is assumed to supported on the roof of the fuselage at four nodes. Set I consists of the four nodes 39, 48, 46 and 37 and Set II consists of nodes 43, 47, 42 and 38. The data for this model is

given in Table 4.

First, a convergence study on the vibratory levels in the fuselage with respect to the number of fuselage modes, was performed. The gearbox is assumed to be attached to the fuselage at nodes given in Set I. Figure 17 presents the results of the convergence study. Inclusion of 20 flexible modes of the fuselage provides good convergence in the vibratory levels at all nodes. The reason for the good convergence is that all the important modes whose natural frequencies are in the neighbourhood of the excitation frequency 4/rev are included in the analysis. This is evident from Table 5 presenting the natural frequncies of the coupled gearbox-fuselage system for the several cases considered in the convergence study. Hence, in all subsequent studies on vibration measurement and control, 20 flexible modes of fuselage are included.

The influence of locations of attachment of the gearbox to the fuselage is also studied. Set I and Set II represent the two cases of connectivity of the gearbox to the fuselage. The vibratory levels at various nodes in the fuselage for these two cases are shown in Fig.18. Set I connectivity provides a higher level of vibration in the fuselage than Set II. Hence, Set I connectivity is chosen as the reference case for vibration minimisation studies described in the following section.

6.3 Open-Loop Vibration Control

For the vibration control studies, the total number of degrees of freedom of the dynamic model is 26. This consists of 3 rigid body degrees of freedom of the gearbox, 3 rigid body degrees of freedom and 20 flexible modes of the fuselage. Since, there are 23 degrees of freedom for the fuselage, 23 sensor locations were identified by EIDV approach employing single elimination process. These optimally selected 23 sensors locations are indicated by node numbers in Fig.19.

Incorporating an open-loop control scheme, described in Chapter 5, an attempt is made to minimise the vibratory response of the fuselage. The control forces, required for vibration minimisation, are evaluated using measurements from several sets of sensor locations. These different sets of sensor locations correspond to (i) optimally placed 23 sensors, (ii) arbitrarily placed 5 sensors(node locations 12, 13, 20, 21 and 64), (iii) arbitrarily placed 10 sensors (node locations 1, 2, 20, 21, 31, 35, 50, 56, 62 and 64) and (iv) arbitrarily placed

23 sensors (node locations 1 through 22 and 64). The gearbox is attached to the fuselage at node locations given in Set I. Assuming a 4-bladed rotor system, the nondimensional frequency of the excitation force is 4/rev. The relevant data are given in Table 4.

Using the g-levels measured at the optimally selected 23 locations, the control forces required for minimisation of vibration in fuselage were calculated. Figure 20 shows a comparison of the baseline vibratory levels along with the controlled response. The fuselage vibratory level has been reduced substantially from the basline peak acceleration of 0.284g to a level of 0.5E-04g at node location 33. In addition, the vibratory levels at all nodes in the fuselage are reduced to very low levels. But the gearbox C.G. experiences an increase in the g-level, i.e., the gearbox g-level increased from a value of 0.0477g to 0.0625g. Figures 21(a) and 21(b) show the magnitudes and the phase angles of the four control forces required for vibration minimisation.The control forces are almost 180 degrees of out-of-phase to the applied external force. This observation can be mathematically proved using a simple two degree of freedom model with a control force generator placed between them, which is described in Appendix C.

To analyse the effectiveness of vibration reduction using optimally placed 23 sensors, a vibration reduction analysis using different sets of sensors located at arbitrary nodes in the fuselage, was performed. The controlled response for these cases of arbitrary sensor locations are compared with the controlled response for the case of 23 optimally placed sensors. These results are shown in Figs.22-24.

Figure 22 shows the results of the controlled vibratory response, obtained using 5 arbitrary sensors and 23 optimally placed sensors. It is observed that the peak acceleration of the controlled response with 5 arbitrary sensors is 0.31E-02g at node location 43. The peak acceleration of the controlled response for optimally placed 23 sensors is 0.138E-03g at node location 5. Figure 23 shows a comparison of the controlled vibration with 10 arbitrary sensors and 23 optimally placed sensors. For the case of 10 arbitrary sensors, the peak acceleration of the controlled response is 0.211E-03g at node location 33, which is about 53% more than that for the case of optimally placed 23 sensors. Figure 24 shows the controlled response for the case of 23 arbitrary sensors along with the controlled response with 23 optimally placed sensors. For the case of 23 arbitrary sensors, the peak acceleration is found to be 0.203E-03g at node location 41, which is 47% more than that for the case of optimally placed 23 sensors. The magnitudes and phase angles of the control

forces for all these case are shown in Figs.(25-27) and are also presented in Table 6. It is interesting to note that though there is very small variation in the magnitudes and phase angles of the control forces, there seems to be a large variation in the peak acceleration of the controlled vibratory response of the fuselage. These results clearly indicate that the vibration control using measurements from the optimally placed sensors provide the minimium peak acceleration in the fuselage. This shows that the EIDV approach with single elimination seems to be an effective technique for identifying the sensor locations for vibration control in helicopters.

It is observed that in all these vibration minimisation studies, even though there is vibration reduction in the fuselage, the gearbox c. g. experiences an increase in the acceleration level (Figs.22-24). So an attempt was made to reduce simultaneously the vibratory levels at the gearbox c. g. as well as at the fuselage. In this case, the control forces required for vibration minimisation were obtained using measurements from 24 sensors (23 optimal sensor locations in the fuselage + 1 sensor at gearbox c. g.). Figure 28 shows the comparison of controlled vibratory levels obtained by using measurements from 23 optimal locations and those for the case of 24 sensors. It is interesting to observe that with 24 sensors there is no improvement in vibratory levels at the gearbox c. g., but there is deterioration in the fuselage vibratory levels. The magnitudes and phase angles of the control forces for the 24 sensors case are shown in Fig.28, and are also given in Table 6.

Chapter 7

CONCLUDING REMARKS

The problem of vibration reduction in helicopter fuselage, using a new concept of Active Control of Structural Response (ACSR), has been formulated. The equations of motion representing the dynamics of a coupled gearbox-fuselage model have been derived. Using these equations, several studies have been performed. They are (i) identification of optimal sensor locations for vibration measurement, (ii) influence of number of flexible modes on the vibratory response of a three dimensional finite element model of a fuselage structure and (iii) formulation and solution of a Multi-Input-Multi-Output (MIMO) control scheme for vibration minimisation in the helicopter fuselage.

The important conclusions of this study are summarised below.

1. A detailed description of the Effective Independence Distribution Vector (EIDV) approach for the identification of sensor locations for vibration measurement is presented. An example problem has been formulated and solved to highlight the essential features of this EIDV approach.

2. With condition number of Fisher Information matrix as a reference parameter, it was observed that the single elimination process provides a condition number which is many orders lower than that corresponding to group elimination process.

3. The condition number of modal matrix is shown to be highly dependent on the normalising factors used for different modal vectors.

4. Irrespective of the input excitation frequency, the optimally identified sensor locations by the single elimination process, experience high levels of vibration.

5. For an excitation frequency of 4/rev, it was observed that 20 flexible modes of fuselage provide a good convergence for the vibratory response of fuselage.

6. Vibration control using measurements from the optimally selected sensor lcoations provide maximum reduction in the g-levels of the fuselage vibration as compared to the controlled response using measurements from arbitrarily placed sensor locations.

7. When the vibratory levels in the fuselage are minimised, the gearbox experiences a higher level of vibration in comparison to the baseline g-level. While trying to minimise simultaneously the vibratory levels in the fuselage and the gearbox, it was observed that there is no reduction in the vibratory levels at gearbox; but there is a deterioration in the control of vibration in the fuselage.

7.1 Scope for Further Work

This study can be further extended to incorporate

- Closed-loop active control methodologies for vibration minimisation
- Inclusion of rotor dynamics in the analysis
- Vibration analysis and minimisation at several flight conditions.

References

1. Reichert, G., 'Helicopter vibration control - a survey', Vertica, Vol. 5, No. 1, 1981, pp. 1-20.

2. Loewy, R.G., 'Helicopter vibrations: A technological perspective', Journal of the American Helicopter Society, Vol. 29, No. 4, Oct. 1984, pp. 4-30.

3. Kvaternik, R.G., Bartlett, F.D.Jr. and Cline, J.H., 'A summary of recent NASA/ ARMY contributions to rotorcraft vibrations and structural dynamics technology', NASA/ ARMY Rotorcraft Technology, NASA CP-2495, 1988.

4. Crews, S.T., 'Rotorcraft vibration criteria : A new perspective', Proceedings of the 43-rd Annual Forum of the American Helicopter Society, St. Louis, May 1987.

5. Huber, H., 'Parameteric trends and optimization - Preliminary selection of configurarion - prototype design and manufacture', Helicopter Aerodynamics and Dynamics, AGARD LS-63, 1973.

6. Wang, B.P., Kitis, L., Pilkey, W.D. and Palazzolo, A.B., 'Helicopter vibration reduction by local structural modification', Journal of the Americal Helicopter Society, Vol. 27, No. 3, July, 1982, pp. 43-47.

7. Gabel, R. and Lang, P., 'CH-47D airframe vibration reduction through airframe stiffening', 51-st Annual Forum of the American Helicopter Society, Fort Worth, TX, May 1995.

8. Friedmann, P.P., 'Helicopter vibration reduction using structural optimisation with aeroelastic/ multidisciplinary constraints - A survey', Journal of aircraft, Vol. 28,

No. 1, 1991, pp. 8-21.

9. Hamouda, M.H. and Pierce, G.A., 'Helicopter vibration suppression using simple pendulam absorbers on the rotor blade', Journal of the American Helicopter Society, Vol. 29, No. 3, July 1984, pp. 19-29.

10. Viswanathan, S.P. and McClure, R.D., 'Analytical and experimental investigation of a bearingless hub absorber', Journal of the American Helicopter Society, Vol. 28, No. 3, July 1983, pp. 45-57.

11. Desjardins, R.A. and Hooper, W.E.,'Helicopter rotor vibration isolation', Vertica, Vol. 8, 1984, pp. 145-159.

12. Braun, D., 'Ground and flight test of a passive rotor isolation system for vibration reduction', Vertica, Vol. 8, 1984, pp. 1-14.

13. Halwes, D.R., 'LIVE-Liquid Inertia Vibration Eliminator', 36-th Annual Forum of the American Helicopter Society, Washington,D.C., May 1980.

14. Sivaramakrishnan, R., Venkatesan, C., and Varadan, T.K., 'Rotor/fuselage vibration isolation studies by a Floquet Harmonic iteration technique', Journal of Aircraft, Vol. 27, No. 1, Jan. 1990.

15. Wood, E.R., Powers, J.H., Cline, J.H. and Hammond, C.E., 'On developing and flight testing a higher harmonic system', Journal of the Americal Helicopter Society, Vol. 30, No. 1, Jan. 1985, pp. 3-20.

16. Miao, W., Kottapalli, S.B.R. and Frye, H.M., 'Flight demonstration of higher harmonic control (HHC) on S-76', 42-nd Annual Forum of the American Helicopter Society, Washington, D.C., June 1986.

17. Shaw, J., Albion, A., Hanker, E.J. and Teal, R., 'Higher harmonic control : Wind tunnel demonstration of fully effective vibratory hub force suppression', Journal of the Americal Helicopter Society, Vol. 34, No. 1, Jan. 1989, pp. 14-25.

18. Polychroniadis, M. and Achache, M., 'Higher harmonic control-Flight tests of an experimental system on the SA 349 research Gazelle', 42-nd Annual Forum of the American Helicopter Society, Washington, D.C., June 1986.

19. Kube, R., ' New aspects of a higher harmonic control of a four bladed hingeless model rotor', 15-th European Rotocraft Forum, Amsterdem, Netherlands, Sept. 1986.

20. Ham, N.D., 'Helicopter individual blade control: Promising technology for future helicopter', 2-nd International Aeromechanics specialists' conference, Bridgeport, CT, Oct. 1986.

21. Friedmann, P.P., and Milliott, T.A., 'Vibration reduction in rotorcraft using active control: A comparison of various approaches', Journal of Guidance,Control, and Dynamics, Vol. 18, No. 4, pp. 664-673.

22. King, S.P. Staple, A.E., 'Minimisation of vibration through active control of structural response', Rotorcraft Design Operations, AGARD CP-423, Oct. 1986.

23. Staple, A.E., 'An evaluation of active control of structural response as a means of reducing helicopter vibration', 15-th European Rotorcraft Forum, Amsterdam, Netherlands, Sept. 1989.

24. Welsh, W.A., von Hardenberg, P.C., von Hardenberg, P.W. and Staple, A.E., 'Test and evaluation of fuselage vibration using Active Control of Structural Responses

(ACSR) optimised to ADS-27', Annual Forum of the American Helicopter Society, Washington, D.C., May 1990.

25. Reichert, G. and Huber, H., 'Active control of helicopter vibration', 4-th workshop on Dynamics and Aeroelastic Stability Modeling of Rotorcraft Systems, University of Maryland, College Park, MD, Nov. 1991.

26. Welsh, W., Fredrickson, C., Rauch, C. and Lyndon, I., 'Flight test on an active vibration control system on the UH-60 black hawk helicopter', 51-st Annual Forum of the American Helicopter Society, Fort Worth, TX, May 1995.

27. Chiu, T. and Friedmann, P.P., 'ACSR system of vibration suppression in coupled helicopter rotor/ flexible fuselage model', 37-th AIAA/ASME/ASCE/AHS/ASC Structures, Structural Dynamics and Materials Conference, Salt Lake City, UT, April 1996.

28. Kammer, D.C., 'Sensor placement for on-orbit modal identification and correlation of large space structures', Journal of Guidance,Control, and Dynamics, Vol. 14, No. 2, Mar-April 1991, pp. 251-259.

29. Lim, T.W., ' Actuator/sensor placement for modal parameter identification of flexible structures', Modal Analysis: The International Journal of Analytical and Experimental Modal Analysis, Vol. 8, No. 1, Jan. 1993, pp. 1-13.

30. Penny, J.E.T., Friswell, M.I. and Garvey, S.D., 'Automatic choice of measurement locations for dynamic testing', AiAA Journal, vol. 32, No. 2, Feb. 1994, pp. 407-414.

31. Kubrusly, C.S. and Malebranche, H., 'Sensors and controllers location in distributed systems- A survey', Automatica, Vol. 21, No. 2, 1985, pp. 117-128.

32. Staley, J.A. and Sciarra, J.J, 'Coupled rotor - airframe vibration prediction methods', Rotorcraft Dynamics, NASA SP-352, 1974.

33. Hohenesmer, K.H. and Yin, S.K., 'The role of rotor impedance in the vibration analysis of rotorcraft', Proceedings of the Fourth European Powered Lift Forum, Stressa, Italy, Sept. 1978.

34. Hsu, T.K. and Peters, D.A., 'Coupled rotor - airframe vibration analysis by a combined harmonic balance impedance matching method', Journal of the American Helicopter Society, Vol. 27, No. 1, Jan. 1982, pp. 25-34.

35. Rutkowski, M.J., 'Assessment of rotor - fuselage coupling on vibration predictions using a simple finite element model', Journal of the American Helicopter Society, Vol. 28, No. 3, July 1983, pp. 20-25.

36. Papavassiliou, I., Friedmann, P.P., and Venkatesan, C., 'Coupled rotor - fuselage vibration reduction using open-loop blade pitch control', Mathematical and Computer Modelling, Vol. 18, No. 3/4, 1993, pp. 131-156.

37. Nilakantan, G.R. and Venugopalan, C.V., 'Structural dynamic characteristics of advanced light helicopter - Validation by analysis and tests', Proceedings of the Tenth National Convention of Aerospace Engineers on Ground Testing of Aerospace Vehicles including Engines, Indian Intitute of Technology, Kanpur, India, Feb. 1995.

38. Venkatesan, C., Tiwari, N. and Mangalick, S., 'Formulation of coupled rotor-gearbox-fuselage dynamics for active vibration control studies', Proceedings of the 5-th National Seminar on Aerospace Structures, Indian Institute of Technology, Bombay, India, Jan. 1996.

39. Mangalick, S., Venkatesan, C. and Kishore, N.N., 'Formulation and dynamic analysis of a helicopter fuselage model', Technical Report : IITK/ AE/ ARDB/ AVCH/826/95/01, Department of Aerospace Engineering, Indian Institue of Technology, Kanpur, May 1995.

40. Garybill, F.A., Matrices with application in statistics, 2-nd Edition, The Wadsworth Statistical/Probability Series, Wadsworth Inc., 1983.

41. Leon, Steven J., Linear algebra with applications, 2-nd Edition, Macmillan Publishing Company, 1986.

Iteration j	$[\phi_S]_j$	$[E]_j$	Lowest E_u	Condition Number
1	$\begin{bmatrix} 1 & 0 & 0 \\ 0 & 1 & 0 \\ 0 & 0 & 1 \\ 2 & 0 & 0 \\ 3 & 0 & 0 \\ 4 & 2 & 0 \end{bmatrix}$	$\frac{1}{86}\begin{bmatrix} 5 & -8 & 0 & 10 & 15 & 4 \\ -8 & 30 & 0 & -16 & -24 & 28 \\ 0 & 0 & 86 & 0 & 0 & 0 \\ 10 & -16 & 0 & 20 & 30 & 8 \\ 15 & -24 & 0 & 30 & 45 & 84 \\ 4 & 28 & 0 & 8 & 12 & 72 \end{bmatrix}$	$\frac{5}{86}$	38
2	$\begin{bmatrix} 0 & 1 & 0 \\ 0 & 0 & 1 \\ 2 & 0 & 0 \\ 3 & 0 & 0 \\ 4 & 2 & 0 \end{bmatrix}$	$\frac{1}{81}\begin{bmatrix} 29 & 0 & -16 & -24 & 26 \\ 0 & 81 & 0 & 0 & 0 \\ -16 & 0 & 20 & 30 & 8 \\ -24 & 0 & 30 & 45 & 12 \\ 26 & 0 & 8 & 12 & 68 \end{bmatrix}$	$\frac{20}{81}$	37
3	$\begin{bmatrix} 0 & 1 & 0 \\ 0 & 0 & 1 \\ 3 & 0 & 0 \\ 4 & 2 & 0 \end{bmatrix}$	$\frac{1}{61}\begin{bmatrix} 25 & 0 & -24 & 18 \\ 0 & 61 & 0 & 0 \\ -24 & 0 & 45 & 12 \\ 18 & 0 & 12 & 52 \end{bmatrix}$	$\frac{25}{61}$	33
4	$\begin{bmatrix} 0 & 0 & 1 \\ 3 & 0 & 0 \\ 4 & 2 & 0 \end{bmatrix}$	$\begin{bmatrix} 1 & 0 & 0 \\ 0 & 1 & 0 \\ 0 & 0 & 1 \end{bmatrix}$	--	33

Table 1. Example Problem

Mode	Natural frequencies of helicopter model	
	Frequencies in Hz	Nondimensional frequencies
1	3.5109	0.6894
2	4.1491	0.8146
3	9.9545	1.9545
4	12.0511	2.3662
5	13.0459	2.5615
6	13.2619	2.6039
7	15.4780	3.0391
8	16.7103	3.2811
9	18.4370	3.6201
10	19.7831	3.8844
11	22.5630	4.4302
12	23.8393	4.6808
13	24.4473	4.8002
14	24.7372	4.8571
15	25.0777	4.9239
16	26.6665	5.2359
17	30.3410	5.9574
18	30.4265	5.9742
19	31.3445	6.1544
20	32.6280	6.4064

Table 2: Natural frequencies of first 20 modes of the baseline configuration of helicopter fuselage

Mode	Natural frequencies	
	Baseline fuselage (Hz)	Modified fuselage (Hz)
1	3.5109	3.5371
2	4.1491	4.1294
3	9.9545	9.8118
4	12.0511	11.7661
5	13.0459	12.9444
6	13.2619	13.2014
7	15.4780	15.2866
8	16.7103	16.6090
9	18.4370	18.2183
10	19.7831	19.9171
11	22.5630	22.5298
12	23.8393	23.9533
13	24.4473	24.4478
14	24.7372	24.5707
15	25.0777	25.0781
16	26.6665	28.1926
17	30.3410	30.3799
18	30.4265	31.1950
19	31.3442	32.3254
20	32.6280	33.9449

Table 3: Natural frequencies of modified helicopter fuselage system along with baseline configuration

Reference quantities for nondimensionalisation

$m_B = 65kg$

$R = 6m$

$\Omega = 32\text{rad/sec}$

Nondimensional quantites:

$K_i = 60.01$

$C_i = 0.033$

$m_F = 33.846$

$m_{GB} = 4.615$

$I_{xxF} = 0.6838$

$I_{yyF} = 2.7350$

$I_{xxGB} = I_{xxGB} = 0.0171$

$\frac{F_z}{M_b \Omega^2 R} = 0.0001$

Location of centre of mass of fuselage from the origion (at nose of the fuselage):

$x = 0.563167$

$y = 0$

$z = 0.083333$

Location of centre of mass of gearbox from the origion (at nose of the fuselage):

$x = 0.563167$

$y = 0$

$z = 0.33333$

Structural damping used for fuselage:

$\beta = 0.005$

Table .4: Data for vibration analysis and control

Mode No.	Nondimensional natural frequencies					
	Rigid Body Modes (RBM)	RBM + 5 modes	RBM + 10 modes	RBM + 15 modes	RBM + 17 modes	RBM + 20 modes
1	7.6932	0.6641	0.6639	0.6639	0.6637	0.6637
2	10.0028	0.8146	0.8145	0.8145	0.8146	0.8146
3	12.3890	2.2913	2.2299	2.2057	2.2004	2.1963
4		2.5082	2.3803	2.3693	2.3121	2.2457
5		2.7589	2.4414	2.3957	2.3851	2.3838
6		7.9603	2.6042	2.6025	2.6020	2.6020
7		10.1363	2.7016	2.6932	2.6529	2.6312
8		12.6932	3.0658	3.0605	3.0594	3.0590
9			3.5981	3.5914	3.4960	3.4744
10			4.6597	3.7922	3.7104	3.7010
11			9.6157	4.4329	4.4303	4.3956
12			10.4418	4.7436	4.4594	4.4291
13			14.5201	4.7761	4.7694	4.7667
14				4.8916	4.7981	4.7981
15				6.1996	4.9236	4.9235
16				9.7430	5.4685	5.4413
17				11.0455	6.5694	5.5312
18				14.7380	11.7584	5.8245
19					11.9704	6.1304
20					15.0572	7.0591
21						11.9308
22						12.3048
23						17.2981

Table 5: Natural frequencies of the coupled gearbox-fuselage system for several idealisations

Control force		Number of sensors used for vibration conrol				
	Node location	5 arbitrary	10 arbitrary	23 optimal	23 arbitrary	24 23 optimal + 1 gearbox c.g.
Magnitude	39	3.756	3.755	3.755	3.755	3.989
	48	3.756	3.756	3.755	3.756	3.561
	46	3.757	3.756	3.755	3.756	3.563
	37	3.756	3.755	3.755	3.755	3.978
Phase angle	39	180.2	180.5	180.4	180.6	180.5
	48	182.4	180.3	180.4	180.3	180.2
	46	178.8	180.3	180.4	180.3	180.2
	37	180.5	180.5	180.4	180.6	180.5

Table 6 Magnitude and phase angle of the control forces

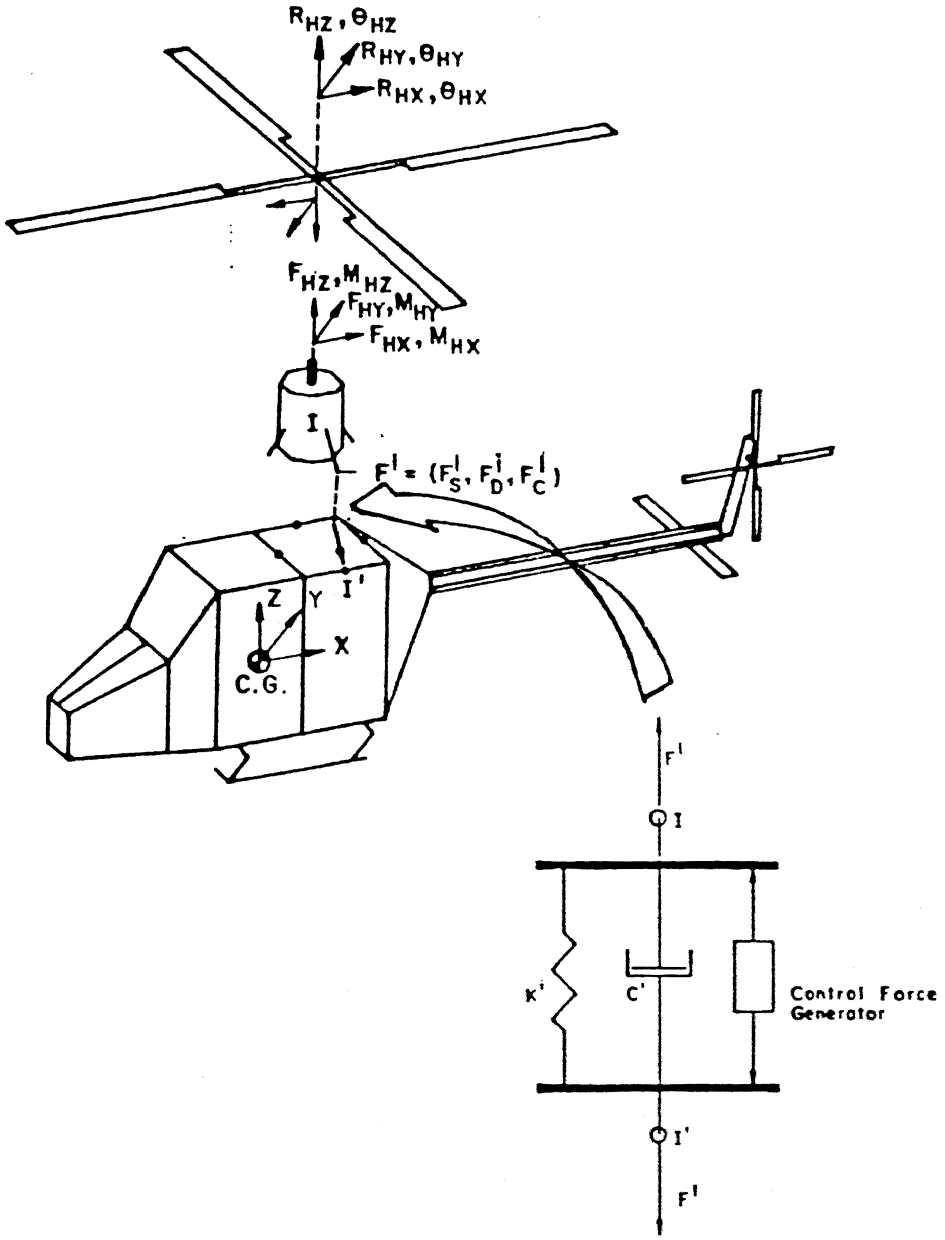

Fig.1 Schematic of helicopter systems interaction

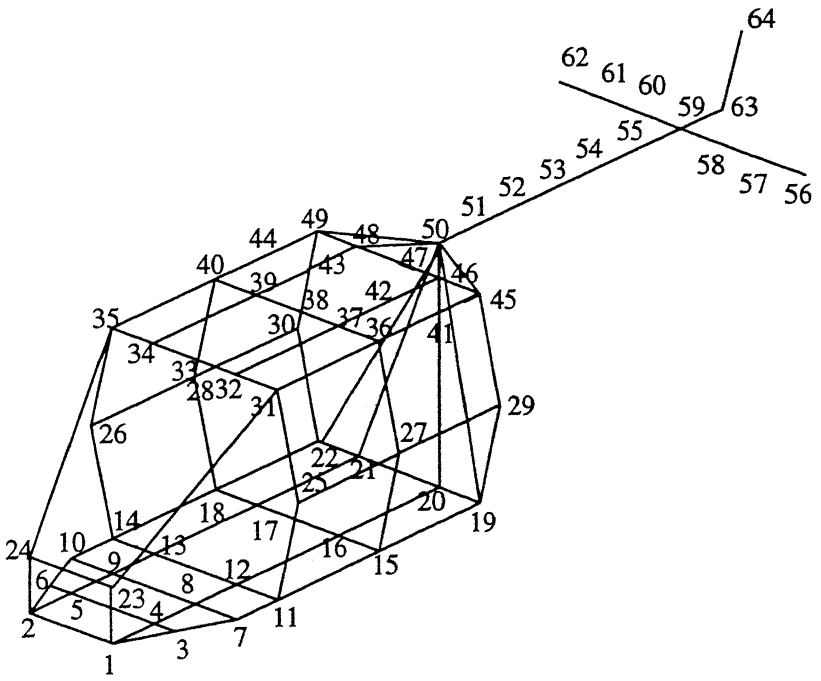

Figure 2: Finite element model of helicopter fuselage

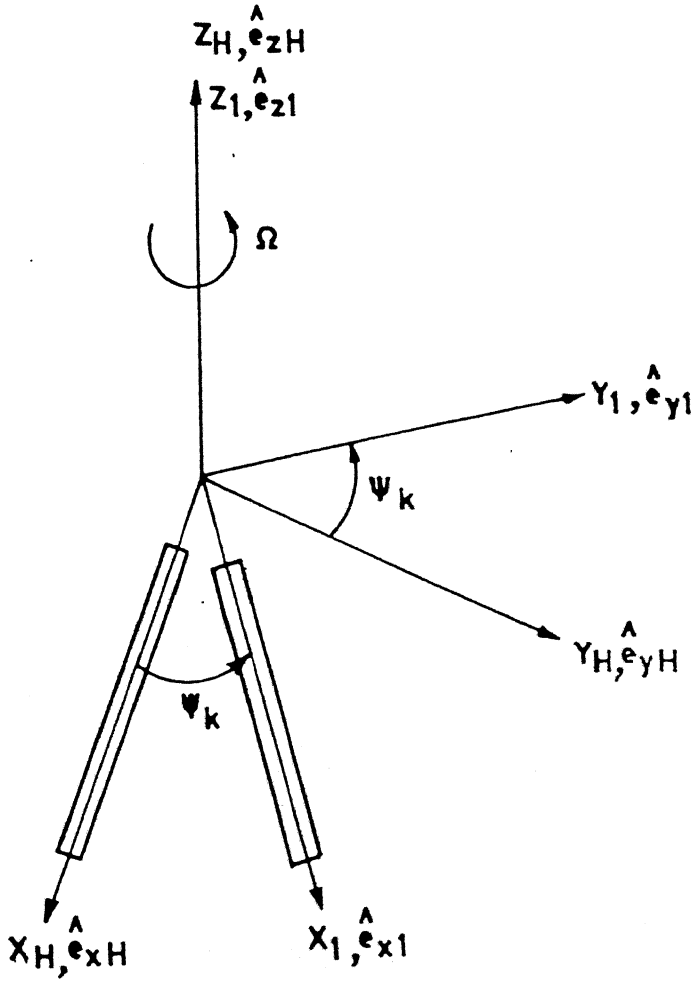

Fig.3 Hub fixed nonrotating and rotating coordinate systems

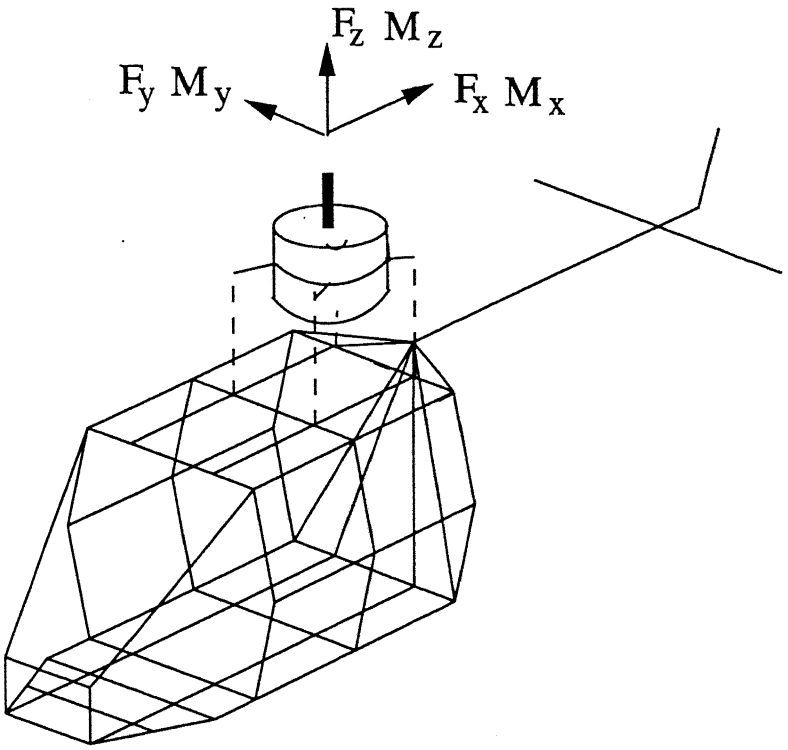

Figure 4: Coupled gearbox-fuselage dynamic model

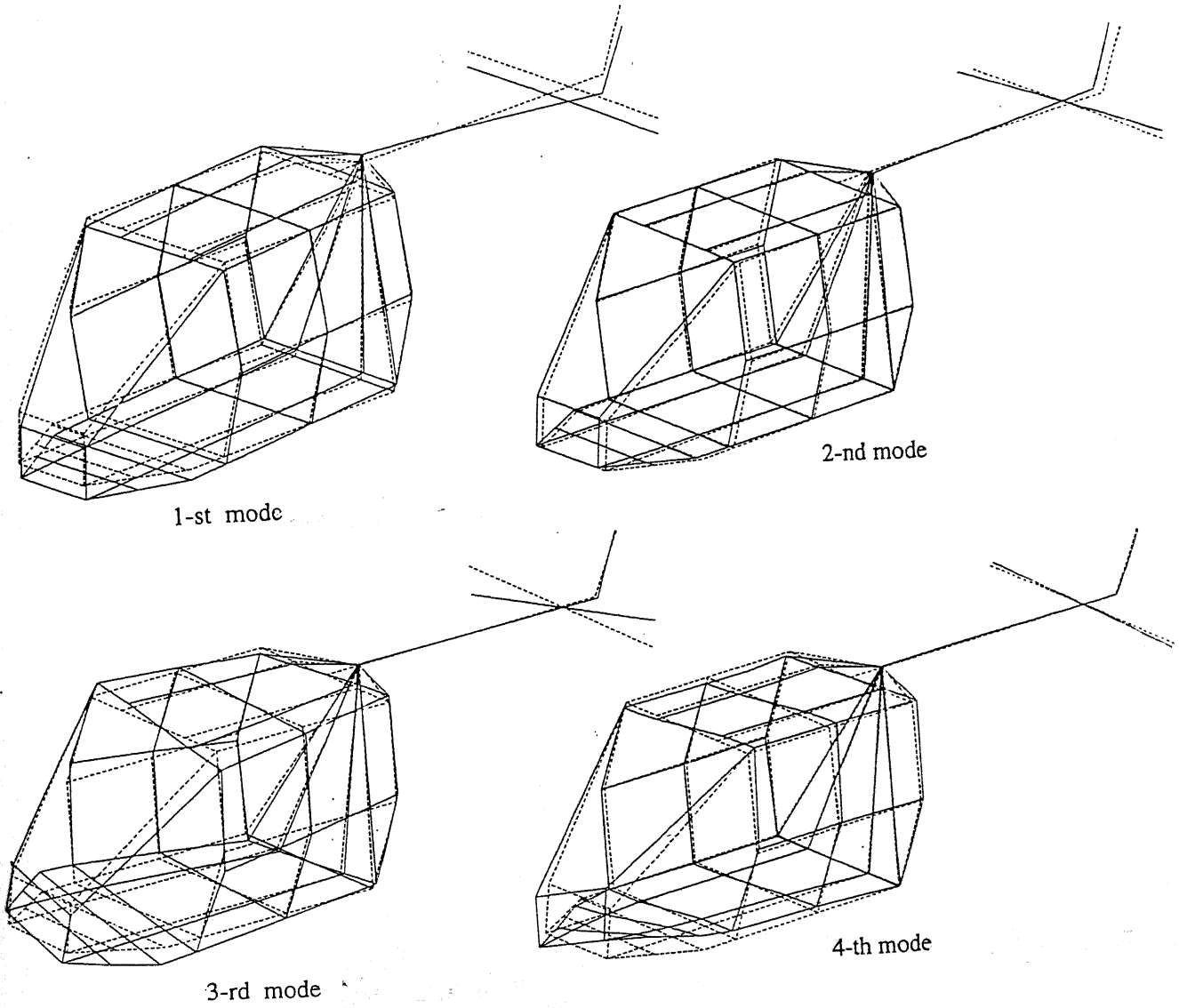

Fig.5 First four mode shapes of the fuselage

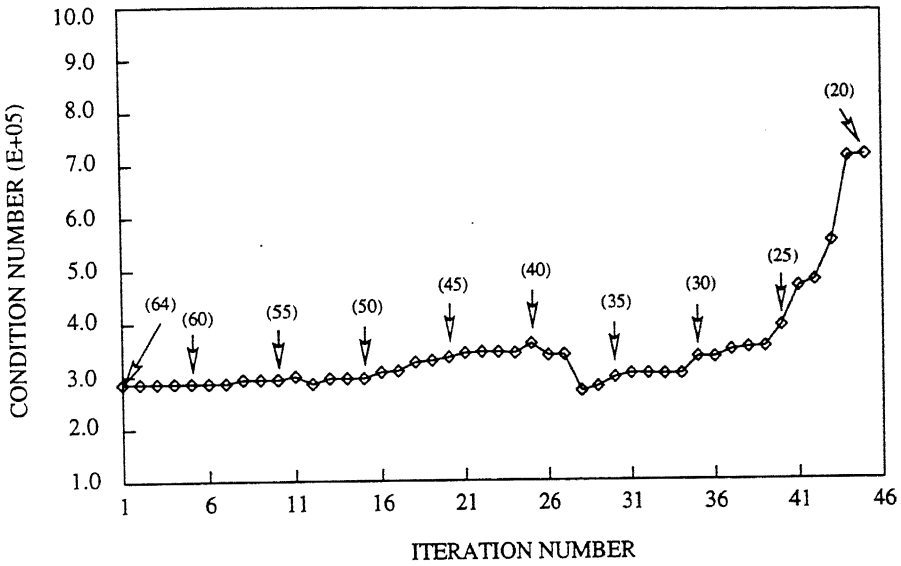

Figure 6: Condition number of Fisher Information Matrix vs iteration number. (Single Elimination)

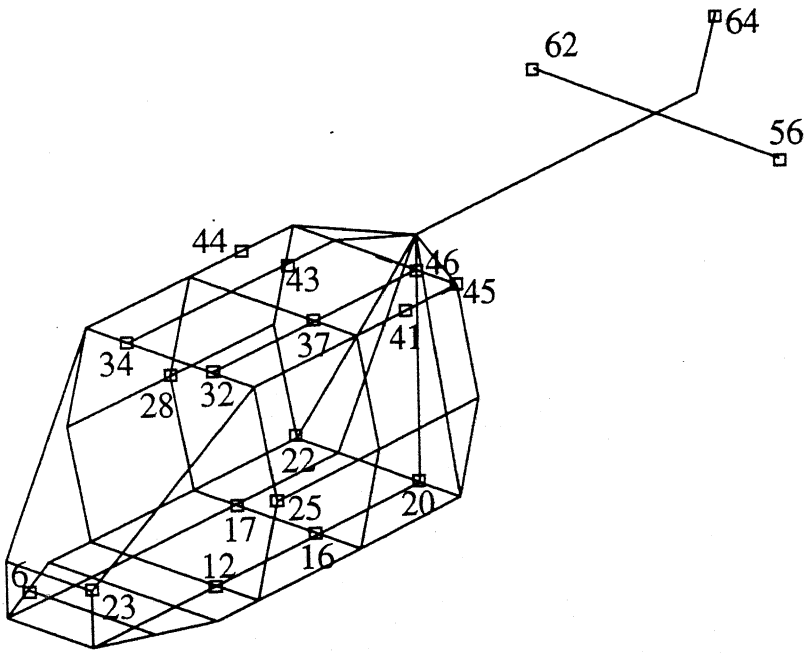

Figure 7: Optimal sensor locations for baseline configuration of the helicopter (20 sensor locations indicated by node numbers)

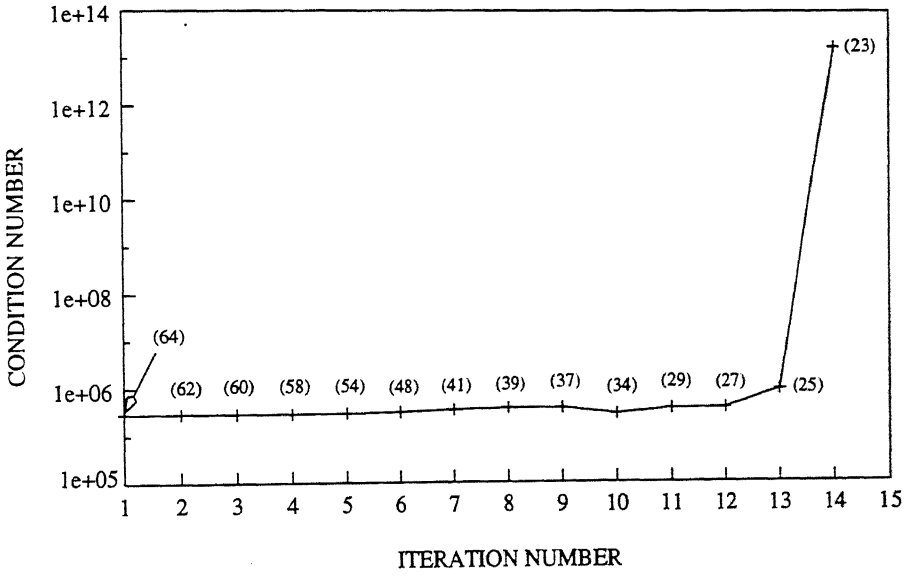

Figure 8: Condition number of Fisher Information Matrix vs iteration number. (Group Elimination)

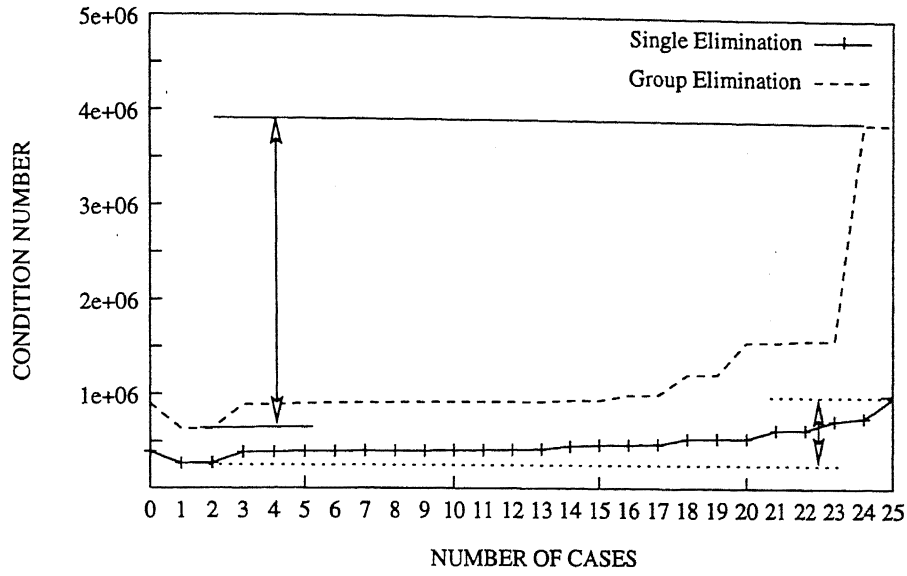

Figure 9: Range of variation of condition number with one sensor failure (Initial set of sensors: 25)

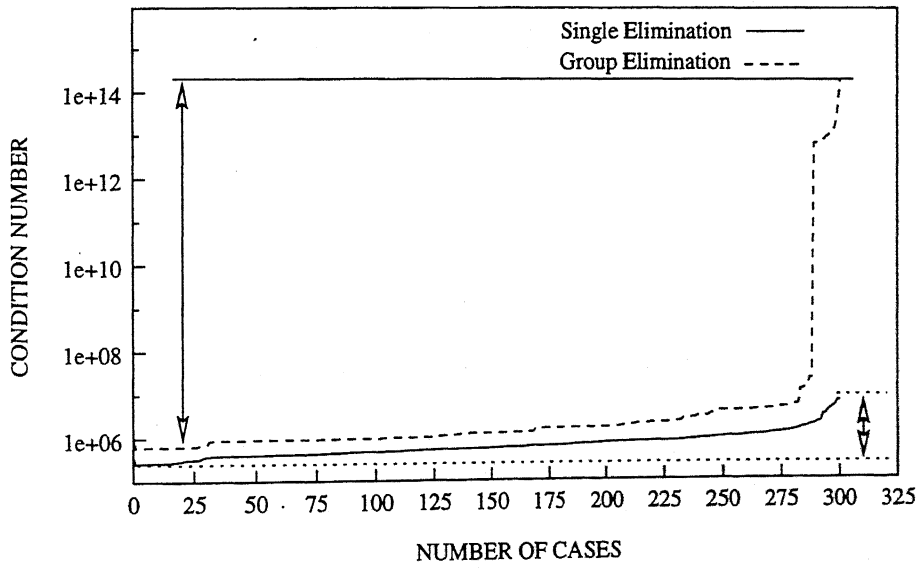

Figure 10: Range of variation of condition number with two sensors failure (Initial set of sensors: 25)

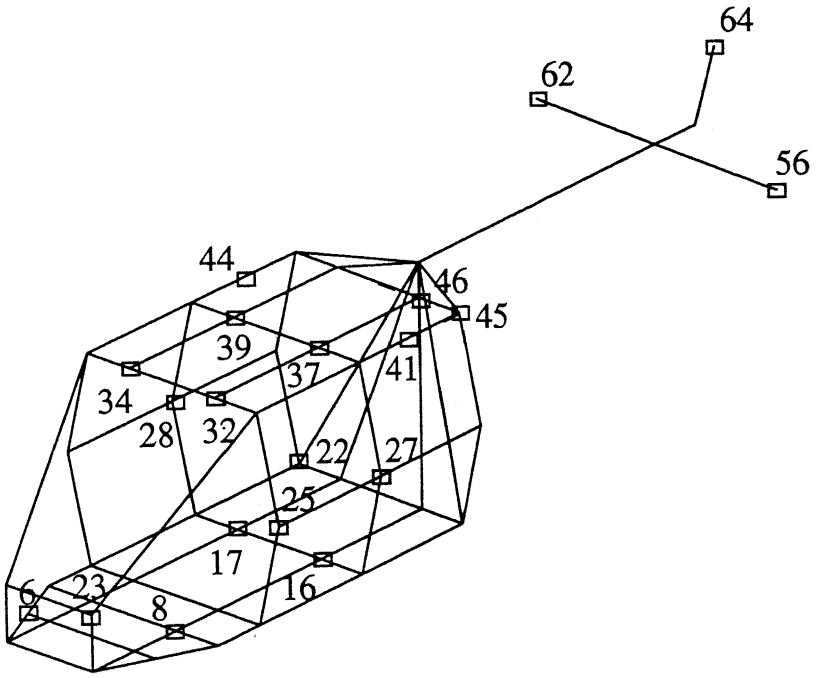

Figure 11: Optimal sensor locations for modified configuration of the helicopter (20 sensor locations indicated by node numbers)

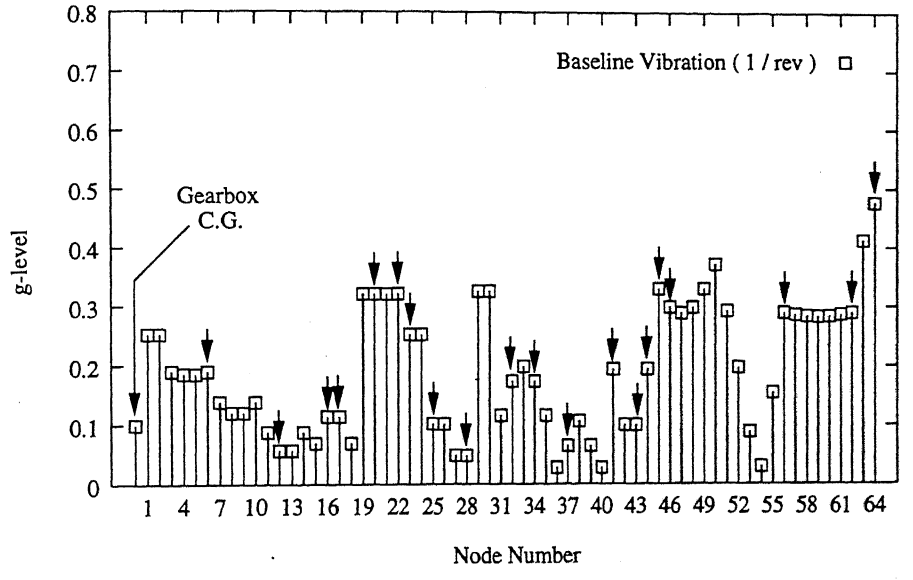

Figure 12: Vibratory response of the fuselage for 1/rev hub force excitation (Optimal sensor locations indicated by arrows)

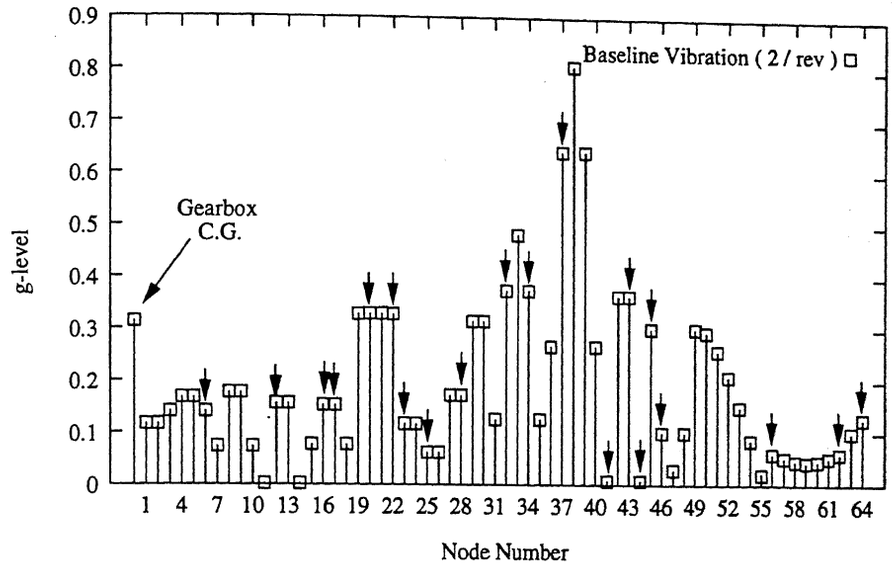

Figure 13: Vibratory response of the fuselage for 2/rev hub force excitation (Optimal sensor locations indicated by arrows)

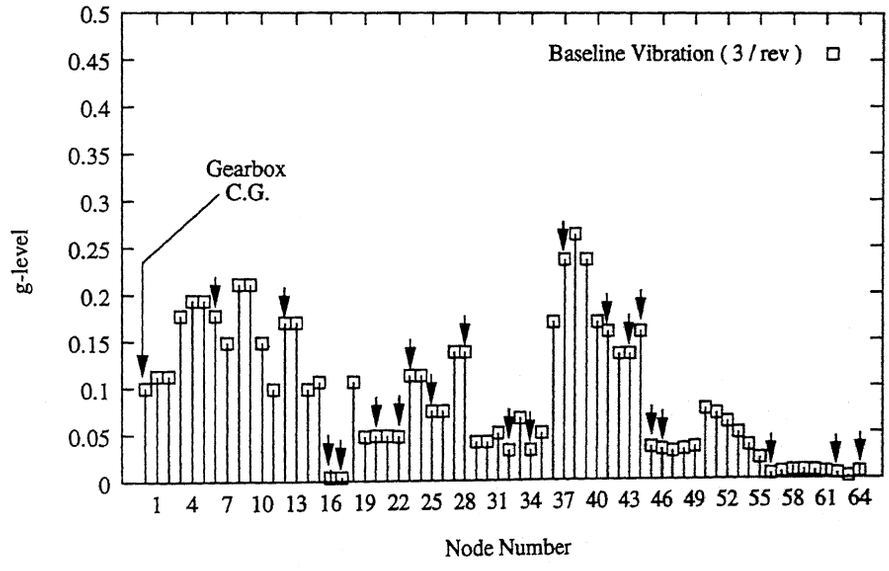

Figure 14: Vibratory response of the fuselage for 3/rev hub force excitation (Optimal sensor locations indicated by arrows)

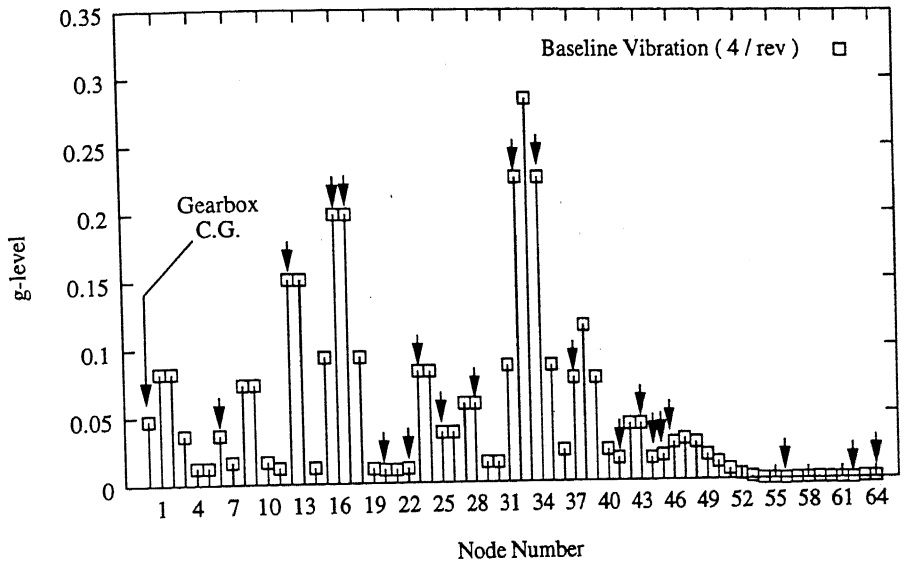

Figure 15: Vibratory response of the fuselage for 4/rev hub force excitation (Optimal sensor locations indicated by arrows)

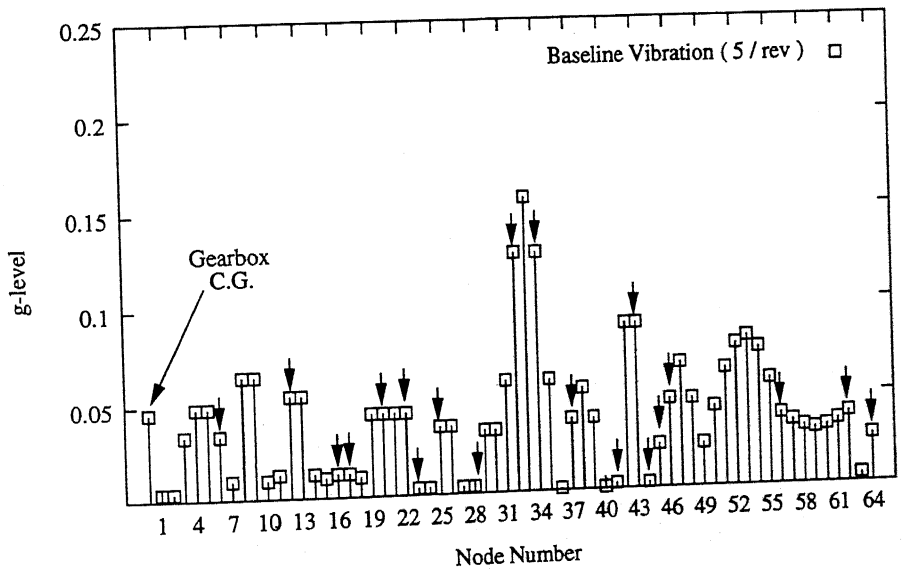

Figure 16: Vibratory response of the fuselage for 5/rev hub force excitation (Optimal sensor locations indicated by arrows)

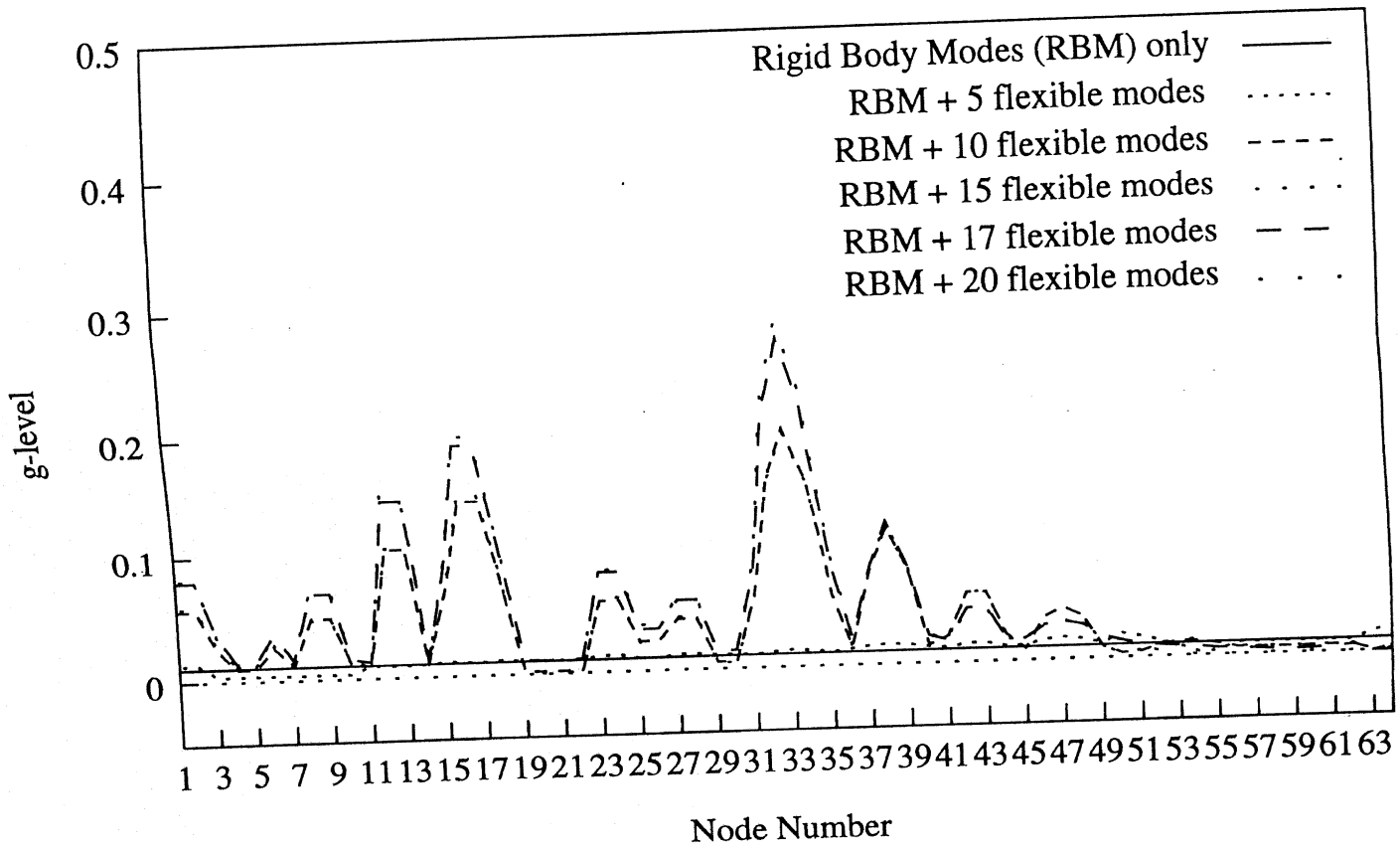

Fig.17 Convergence of vibratory levels in the fuselage w.r.t number of fuselage modes

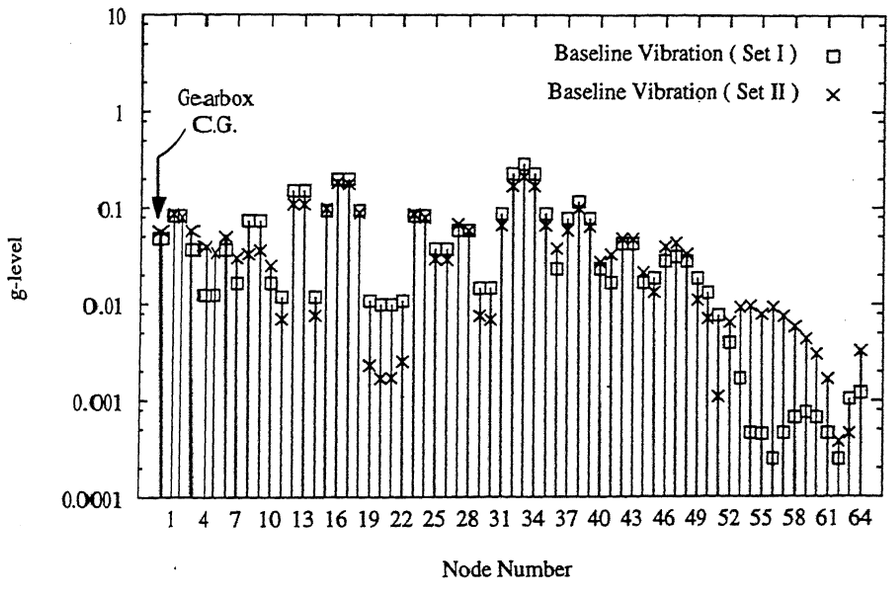

Figure 18: Comparison of vibratory response for two sets of connectivity of gearbox to fuselage (Set I - nodes 39,48,46,37, Set II - nodes 43,47,42,38)

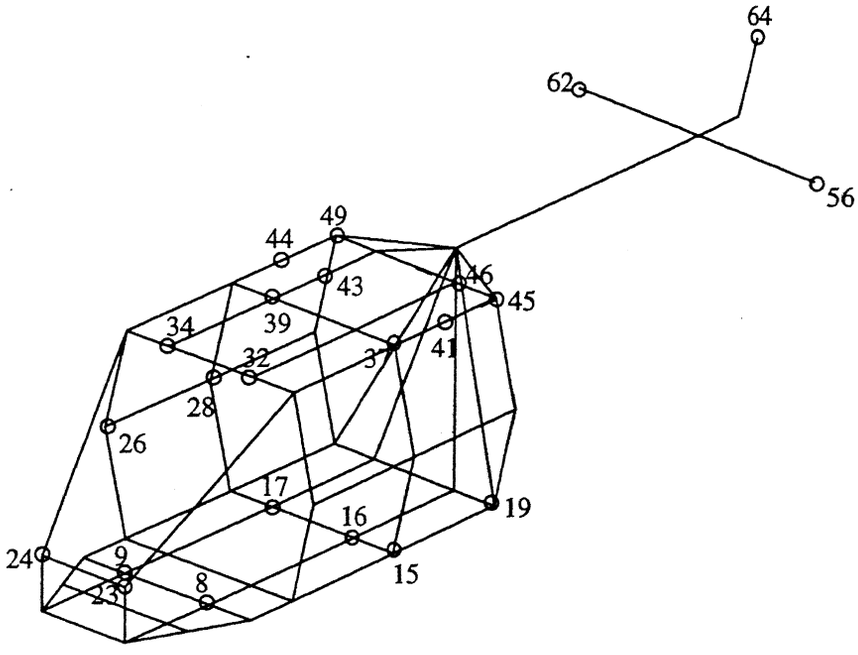

Figure 19: Optimal sensor locations for baseline configuration of the helicopter (23 sensor locations indicated by node numbers)

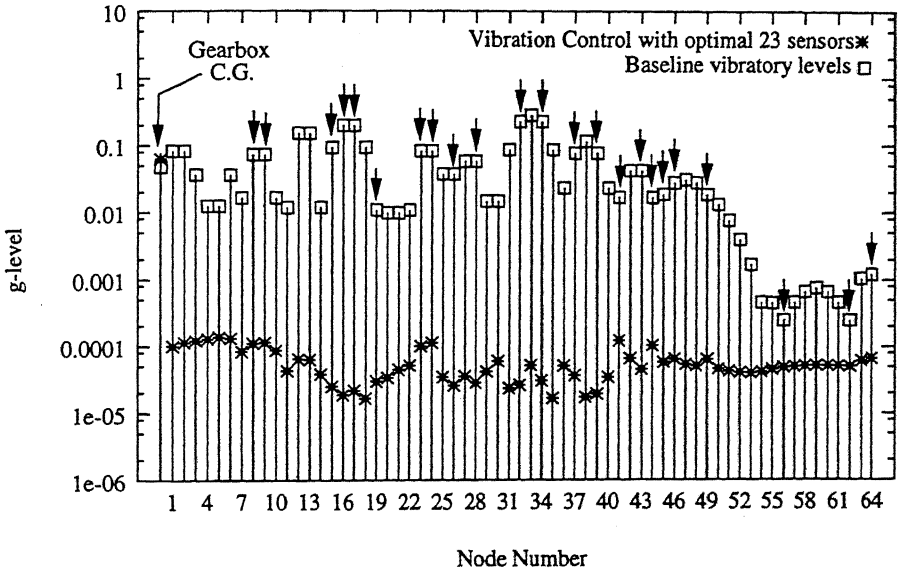

Figure 20: Comparison of baseline and controlled vibratory levels (Optimal sensor locations indicated by arrows)

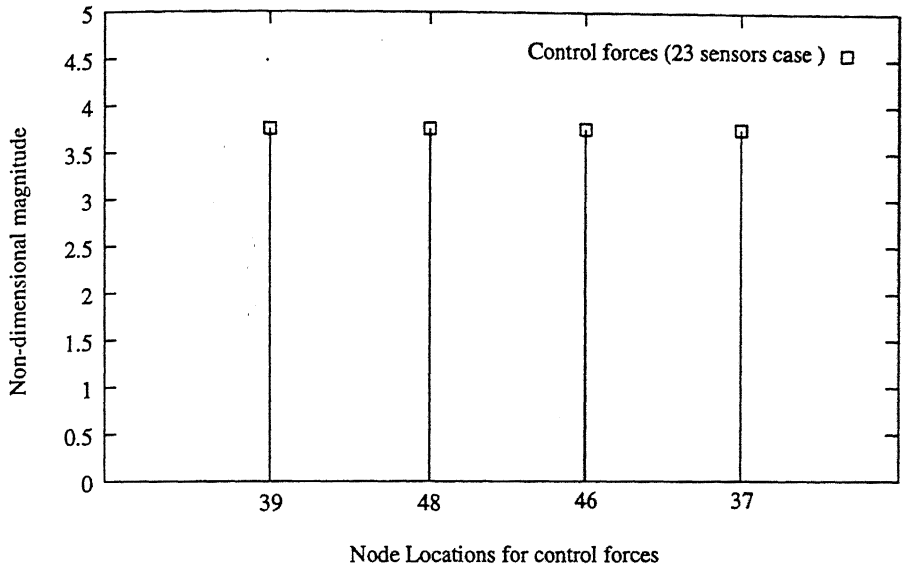

(a)Magnitude

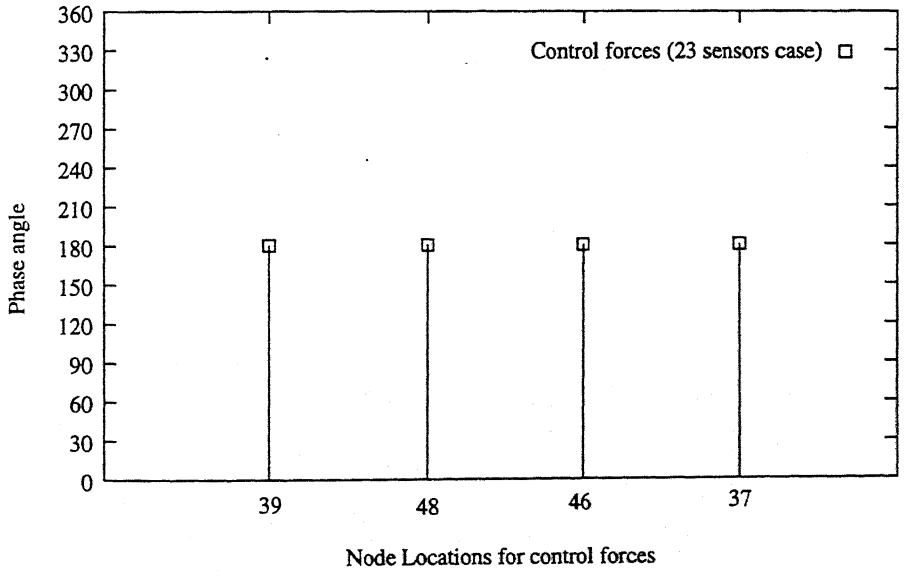

(b)Phase angle

Figure 21: Magnitude and phase angle of control forces for 23 optimal sensor locations

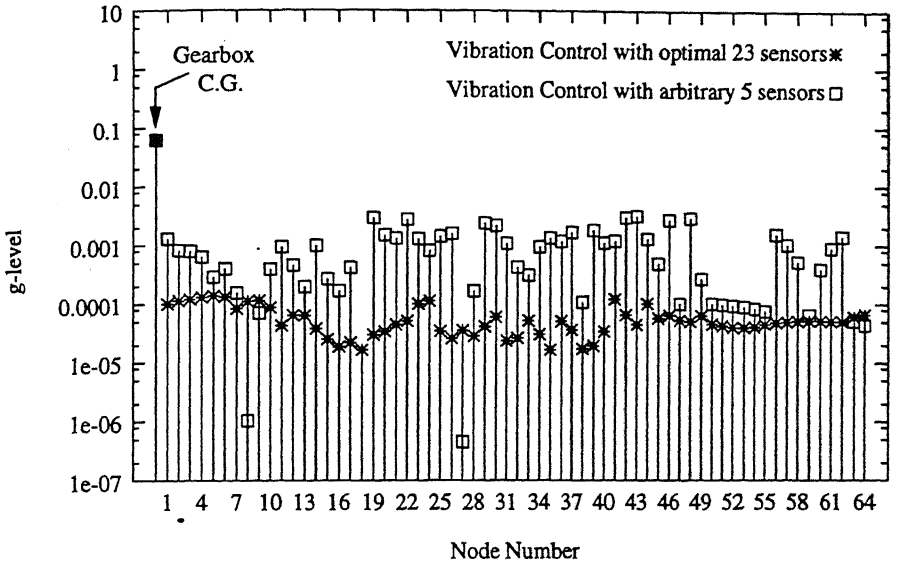

Figure 22: Effectiveness of vibration control with 23 optimal sensors w.r.t vibration control with arbitrary 5 sensors

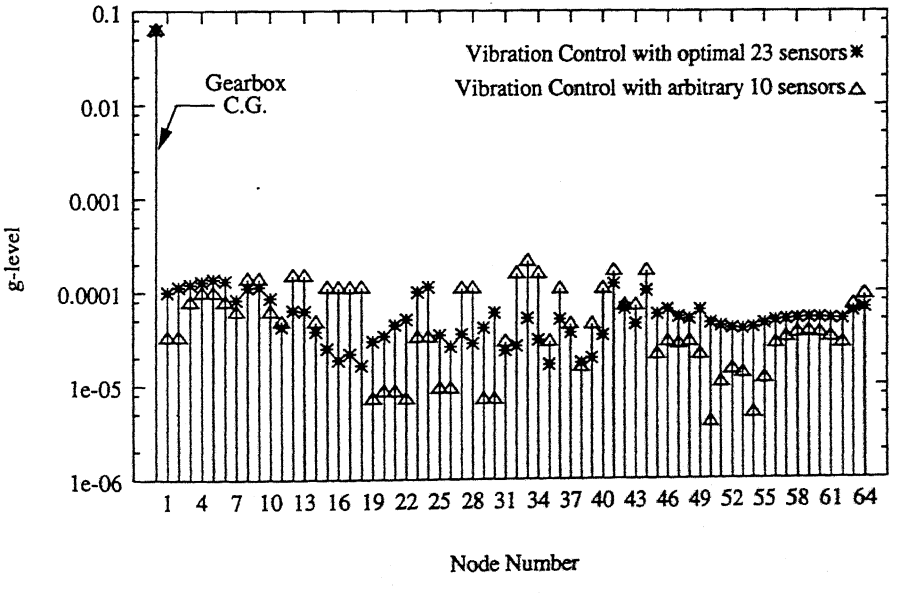

Figure 23: Effectiveness of vibration control with 23 optimal sensors w.r.t vibration control with arbitrary 10 sensors

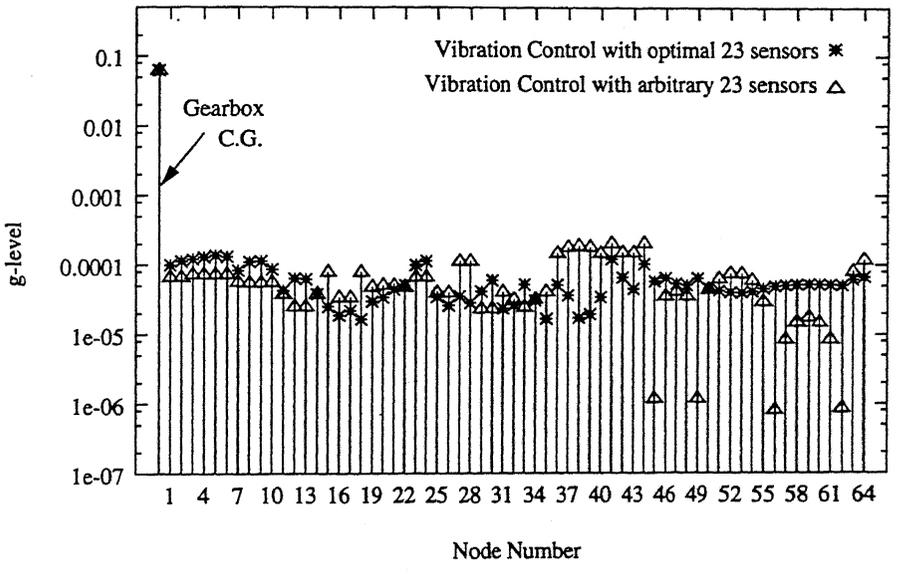

Figure 24: Effectiveness of vibration control with 23 optimal sensors w.r.t vibration control with arbitrary 23 sensors

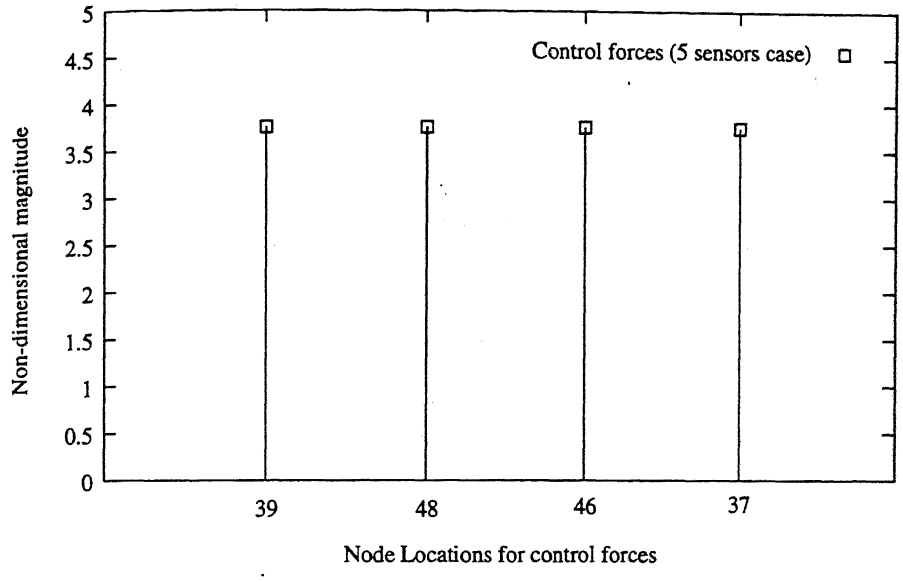

(a)Magnitude

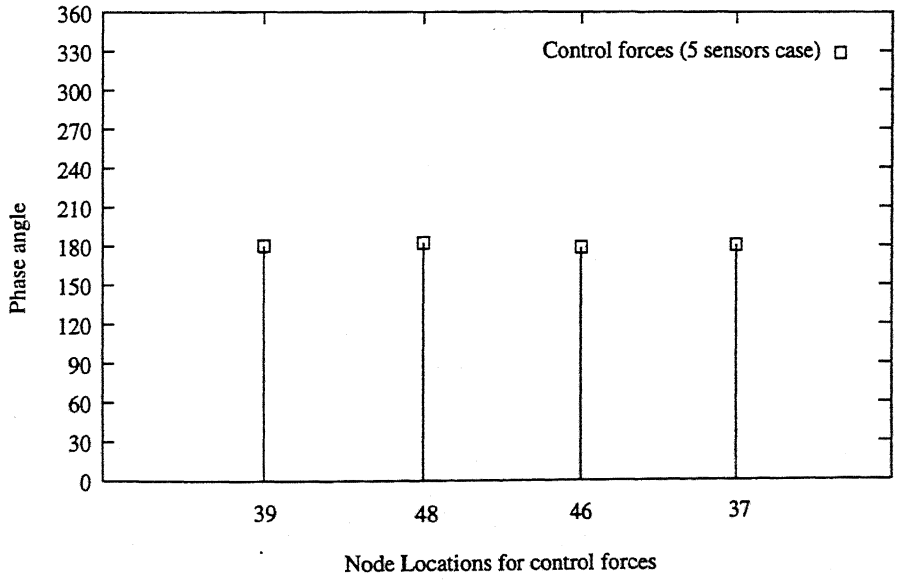

(b)Phase angle

Figure 25: Magnitude and phase angle of control forces for abritrary 5 sensors

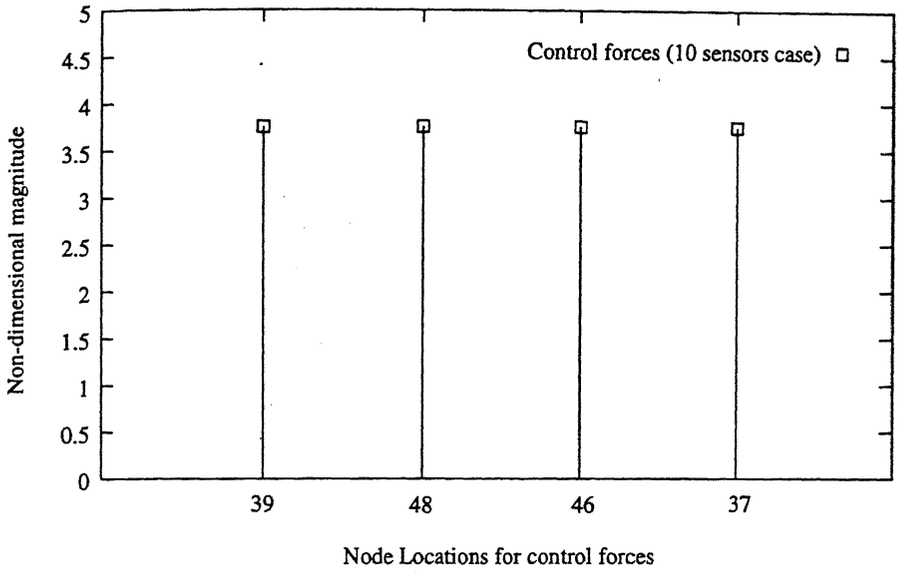

(a)Magnitude

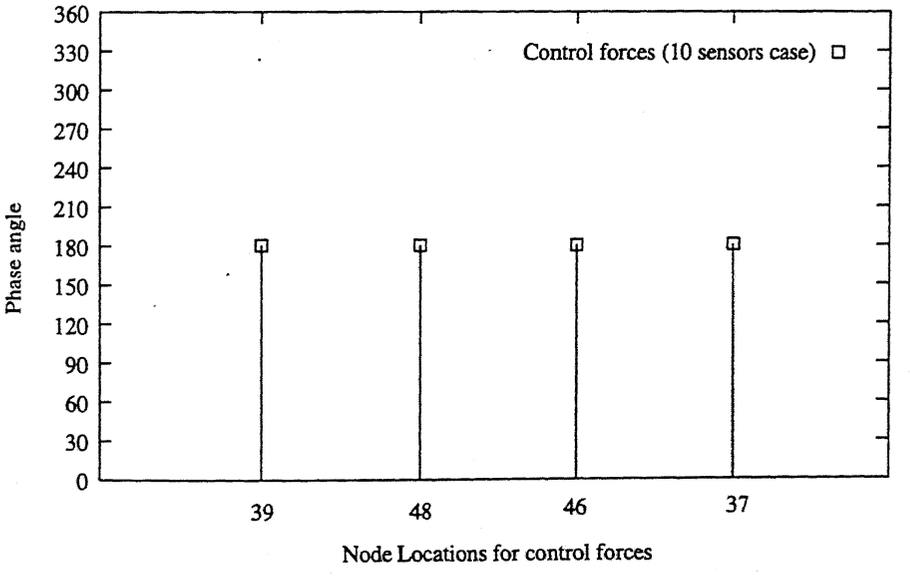

(b)Phase angle

Figure 26: Magnitude and phase angle of control forces for abritrary 10 sensors

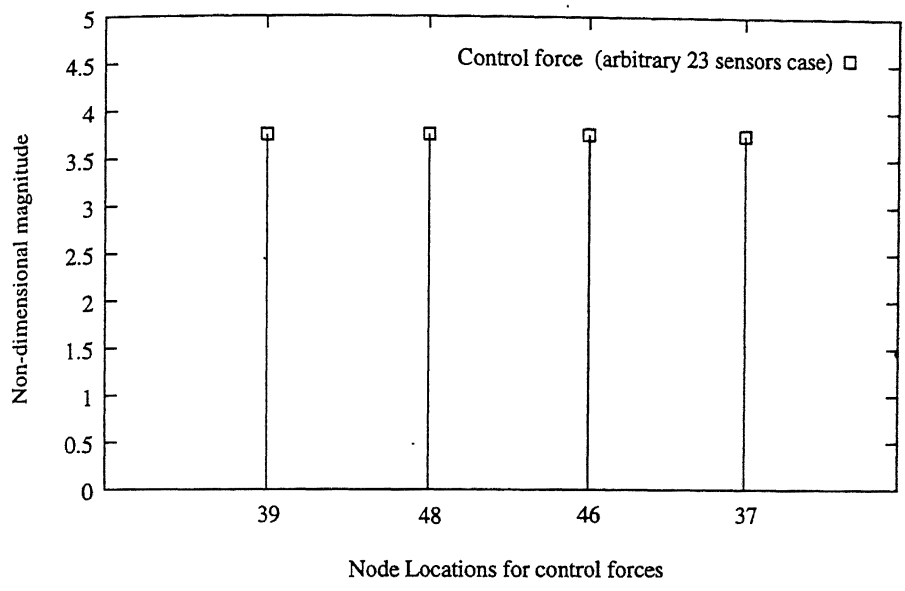

(a)Magnitude

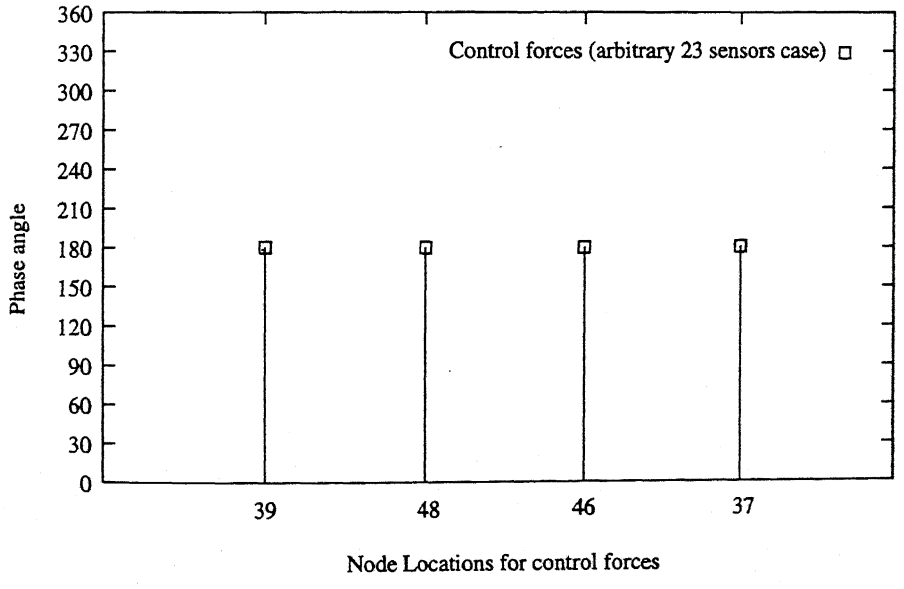

(b)Phase angle

Figure 27: Magnitude and phase angle of control forces for abritrary 23 sensors

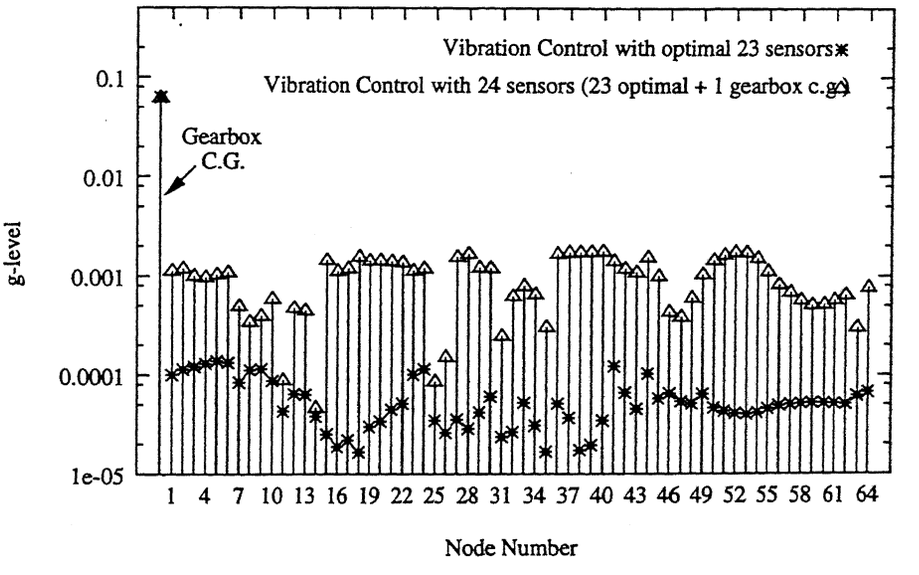

Figure 28: Effectiveness of vibration control with 23 optimal sensors w.r.t vibration control with 24 sensors

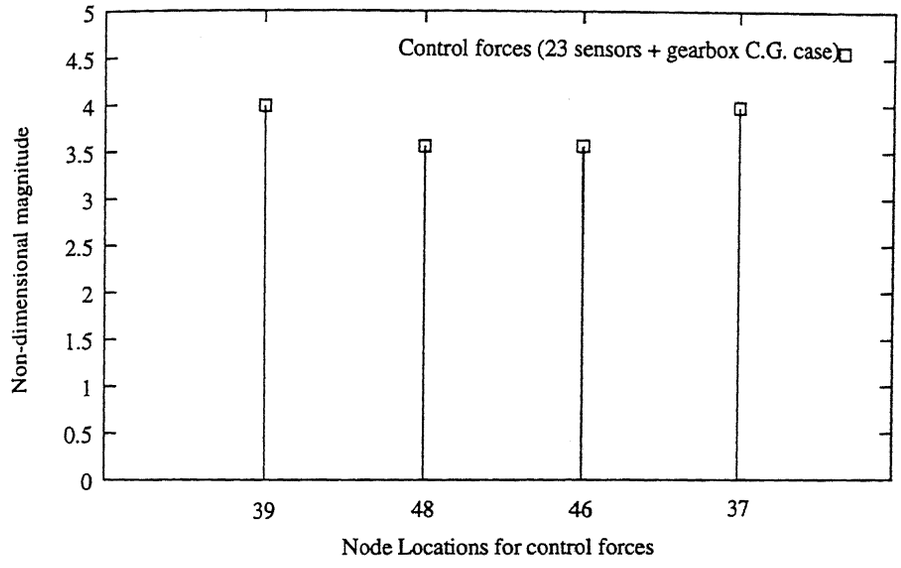

(a)Magnitude

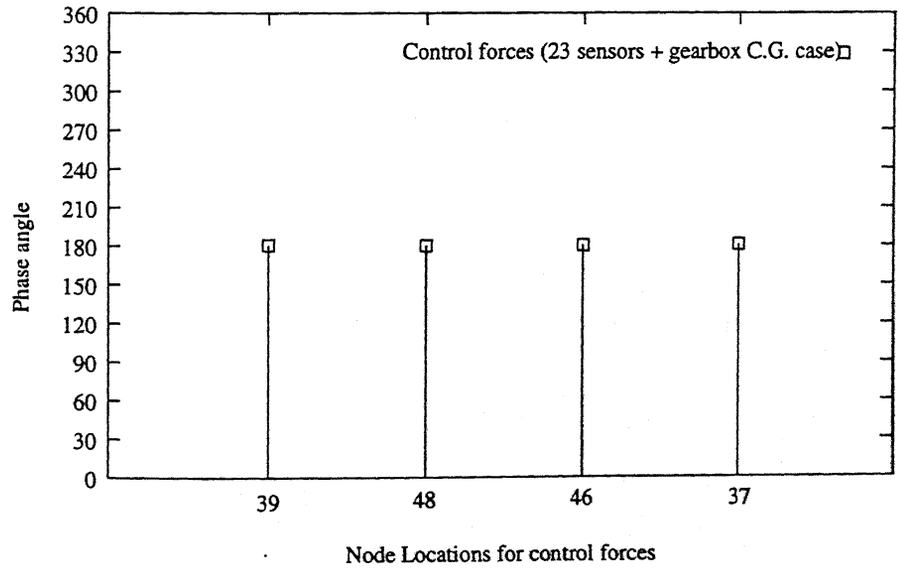

(b)Phase angle

Figure 29: Magnitude and phase angle of control forces for 24 sensors

Appendix A

System matrices [A],[B] and [C]

$$\left[\ A\ \right] = \begin{bmatrix} \{0\} & \vdots & I \\ \cdots & \cdots & \cdots \\ a_1 & \vdots & a_2 \\ a_3 & \vdots & a_4 \\ a_5 & \vdots & a_6 \end{bmatrix}_{2(6+Nm)\times 2(6+Nm)}$$

$$\left[\ a_1\ \right] = \left[\ a_{11}\ \ a_{12}\ \ a_{13}\ \right]$$

$$\left[\ a_2\ \right] = \left[\ a_{21}\ \ a_{22}\ \ a_{23}\ \right]$$

$$\left[\ a_3\ \right] = \left[\ a_{31}\ \ a_{32}\ \ a_{33}\ \right]$$

$$\left[\ a_4\ \right] = \left[\ a_{41}\ \ a_{42}\ \ a_{43}\ \right]$$

$$\left[\ a_5\ \right] = \left[\ a_{51}\ \ a_{52}\ \ a_{53}\ \right]$$

$$\left[\ a_6\ \right] = \left[\ a_{61}\ \ a_{62}\ \ a_{63}\ \right]$$

$$\left[a_{11} \right] = \begin{bmatrix} \frac{1}{m_{GB}}\{-\sum_{i=1}^{NC} K_i & \sum_{i=1}^{NC} K_i p_{xi} & -\sum_{i=1}^{NC} K_i p_{yi}\} \\ \frac{1}{I_{yyGB}}\{\sum_{i=1}^{NC} K_i p_{xi} & -\sum_{i=1}^{NC} K_i {p^2}_{xi} & \sum_{i=1}^{NC} K_i p_{yi} p_{xi}\} \\ \frac{1}{I_{xxGB}}\{-\sum_{i=1}^{NC} K_i p_{yi} & \sum_{i=1}^{NC} K_i p_{xi} p_{yi} & -\sum_{i=1}^{NC} K_i {p^2}_{yi}\} \end{bmatrix}_{3\times 3}$$

$$\left[a_{12} \right] = \begin{bmatrix} \frac{1}{m_{GB}}\{\sum_{i=1}^{NC} K_i & -\sum_{i=1}^{NC} K_i h_{xi} & \sum_{i=1}^{NC} K_i h_{yi}\} \\ \frac{1}{I_{yyGB}}\{-\sum_{i=1}^{NC} K_i p_{xi} & \sum_{i=1}^{NC} K_i h_{xi} p_{xi} & -\sum_{i=1}^{NC} K_i h_{yi} p_{xi}\} \\ \frac{1}{I_{xxGB}}\{\sum_{i=1}^{NC} K_i p_{yi} & -\sum_{i=1}^{NC} K_i h_{xi} p_{yi} & \sum_{i=1}^{NC} K_i h_{yi} p_{yi}\} \end{bmatrix}_{3\times 3}$$

$$\left[a_{13} \right] = \begin{bmatrix} \frac{1}{m_{GB}}\{\sum_{i=1}^{NC} {\Psi^i}_{1z} K_i & \sum_{i=1}^{NC} {\Psi^i}_{2z} K_i & \cdots & \sum_{i=1}^{NC} {\Psi^i}_{Nmz} K_i\} \\ \frac{1}{I_{yyGB}}\{-\sum_{i=1}^{NC} {\Psi^i}_{1z} K_i p_{xi} & -\sum_{i=1}^{NC} {\Psi^i}_{2z} K_i p_{xi} & \cdots & -\sum_{i=1}^{NC} {\Psi^i}_{Nmz} K_i p_{xi}\} \\ \frac{1}{I_{xxGB}}\{\sum_{i=1}^{NC} {\Psi^i}_{1z} K_i p_{yi} & \sum_{i=1}^{NC} {\Psi^i}_{2z} K_i p_{yi} & \cdots & \sum_{i=1}^{NC} {\Psi^i}_{Nmz} K_i p_{yi}\} \end{bmatrix}_{3\times Nm}$$

$$\left[a_{21} \right] = \begin{bmatrix} \frac{1}{m_{GB}}\{-\sum_{i=1}^{NC} C_i & \sum_{i=1}^{NC} C_i p_{xi} & -\sum_{i=1}^{NC} C_i p_{yi}\} \\ \frac{1}{I_{yyGB}}\{\sum_{i=1}^{NC} C_i p_{xi} & -\sum_{i=1}^{NC} C_i {p^2}_{xi} & \sum_{i=1}^{NC} C_i p_{yi} p_{xi}\} \\ \frac{1}{I_{xxGB}}\{-\sum_{i=1}^{NC} C_i p_{yi} & \sum_{i=1}^{NC} C_i p_{xi} p_{yi} & -\sum_{i=1}^{NC} C_i {p^2}_{yi}\} \end{bmatrix}_{3\times 3}$$

$$\left[a_{22} \right] = \begin{bmatrix} \frac{1}{m_{GB}}\{\sum_{i=1}^{NC} C_i & -\sum_{i=1}^{NC} C_i h_{xi} & \sum_{i=1}^{NC} C_i h_{yi}\} \\ \frac{1}{I_{yyGB}}\{-\sum_{i=1}^{NC} C_i p_{xi} & \sum_{i=1}^{NC} C_i h_{xi} p_{xi} & -\sum_{i=1}^{NC} C_i h_{yi} p_{xi}\} \\ \frac{1}{I_{xxGB}}\{\sum_{i=1}^{NC} C_i p_{yi} & -\sum_{i=1}^{NC} C_i h_{xi} p_{yi} & \sum_{i=1}^{NC} C_i h_{yi} p_{yi}\} \end{bmatrix}_{3\times 3}$$

$$\left[a_{23} \right] = \begin{bmatrix} \frac{1}{m_{GB}}\{\sum_{i=1}^{NC} {\Psi^i}_{1z} C_i & \sum_{i=1}^{NC} {\Psi^i}_{2z} C_i & \cdots & \sum_{i=1}^{NC} {\Psi^i}_{Nmz} C_i\} \\ \frac{1}{I_{yyGB}}\{-\sum_{i=1}^{NC} {\Psi^i}_{1z} C_i p_{xi} & -\sum_{i=1}^{NC} {\Psi^i}_{2z} C_i p_{xi} & \cdots & -\sum_{i=1}^{NC} {\Psi^i}_{Nmz} C_i p_{xi}\} \\ \frac{1}{I_{xxGB}}\{\sum_{i=1}^{NC} {\Psi^i}_{1z} C_i p_{yi} & \sum_{i=1}^{NC} {\Psi^i}_{2z} C_i p_{yi} & \cdots & \sum_{i=1}^{NC} {\Psi^i}_{Nmz} C_i p_{yi}\} \end{bmatrix}_{3\times Nm}$$

$$\left[a_{31} \right] = \left[\begin{array}{ccc} \frac{1}{m_F}\{\sum_{i=1}^{NC} K_i & -\sum_{i=1}^{NC} K_i p_{xi} & \sum_{i=1}^{NC} K_i p_{yi}\} \\ \frac{1}{I_{yy_F}}\{-\sum_{i=1}^{NC} K_i h_{xi} & \sum_{i=1}^{NC} K_i p_{xi} h_{xi} & -\sum_{i=1}^{NC} K_i p_{yi} h_{xi}\} \\ \frac{1}{I_{xx_F}}\{\sum_{i=1}^{NC} K_i h_{yi} & -\sum_{i=1}^{NC} K_i p_{xi} h_{yi} & \sum_{i=1}^{NC} K_i p_{yi} h_{yi}\} \end{array} \right]_{3\times 3}$$

$$\left[a_{32} \right] = \left[\begin{array}{ccc} \frac{1}{m_F}\{-\sum_{i=1}^{NC} K_i & \sum_{i=1}^{NC} K_i h_{xi} & -\sum_{i=1}^{NC} K_i h_{yi}\} \\ \frac{1}{I_{yy_F}}\{\sum_{i=1}^{NC} K_i h_{xi} & -\sum_{i=1}^{NC} K_i {h^2}_{xi} & \sum_{i=1}^{NC} K_i h_{yi} h_{xi}\} \\ \frac{1}{I_{xx_F}}\{-\sum_{i=1}^{NC} K_i h_{yi} & \sum_{i=1}^{NC} K_i h_{xi} h_{yi} & -\sum_{i=1}^{NC} K_i {h^2}_{yi}\} \end{array} \right]_{3\times 3}$$

$$\left[a_{33} \right] = \left[\begin{array}{cccc} \frac{1}{m_F}\{-\sum_{i=1}^{NC} {\Psi^i}_{1z} K_i & -\sum_{i=1}^{NC} {\Psi^i}_{2z} K_i & \cdots & -\sum_{i=1}^{NC} {\Psi^i}_{Nmz} K_i\} \\ \frac{1}{I_{yy_F}}\{\sum_{i=1}^{NC} {\Psi^i}_{1z} K_i h_{xi} & \sum_{i=1}^{NC} {\Psi^i}_{2z} K_i h_{xi} & \cdots & \sum_{i=1}^{NC} {\Psi^i}_{Nmz} K_i h_{xi}\} \\ \frac{1}{I_{xx_F}}\{-\sum_{i=1}^{NC} {\Psi^i}_{1z} K_i h_{yi} & -\sum_{i=1}^{NC} {\Psi^i}_{2z} K_i h_{yi} & \cdots & -\sum_{i=1}^{NC} {\Psi^i}_{Nmz} K_i h_{yi}\} \end{array} \right]_{3\times Nm}$$

$$
a_{41}\Big] = \begin{bmatrix} \frac{1}{m_F}\{\sum_{i=1}^{NC} C_i & -\sum_{i=1}^{NC} C_i p_{xi} & \sum_{i=1}^{NC} C_i p_{yi}\} \\ \frac{1}{I_{yyF}}\{-\sum_{i=1}^{NC} C_i h_{xi} & \sum_{i=1}^{NC} C_i p_{xi} h_{xi} & -\sum_{i=1}^{NC} C_i p_{yi} h_{xi}\} \\ \frac{1}{I_{xxF}}\{\sum_{i=1}^{NC} C_i h_{yi} & -\sum_{i=1}^{NC} C_i p_{xi} h_{yi} & \sum_{i=1}^{NC} C_i p_{yi} h_{yi}\} \end{bmatrix}_{3\times 3}
$$

$$
a_{42}\Big] = \begin{bmatrix} \frac{1}{m_F}\{-\sum_{i=1}^{NC} C_i & \sum_{i=1}^{NC} C_i h_{xi} & -\sum_{i=1}^{NC} C_i h_{yi}\} \\ \frac{1}{I_{yyF}}\{\sum_{i=1}^{NC} C_i h_{xi} & -\sum_{i=1}^{NC} C_i h^2{}_{xi} & \sum_{i=1}^{NC} C_i h_{yi} h_{xi}\} \\ \frac{1}{I_{xxF}}\{-\sum_{i=1}^{NC} C_i h_{yi} & \sum_{i=1}^{NC} C_i h_{xi} h_{yi} & -\sum_{i=1}^{NC} C_i h^2{}_{yi}\} \end{bmatrix}_{3\times 3}
$$

$$
\left[a_{43}\right] = \begin{bmatrix} \frac{1}{m_F}\{-\sum_{i=1}^{NC} \Psi^i{}_{1z} C_i & -\sum_{i=1}^{NC} \Psi^i{}_{2z} C_i & \cdots & -\sum_{i=1}^{NC} \Psi^i{}_{Nmz} C_i\} \\ \frac{1}{I_{yyF}}\{\sum_{i=1}^{NC} \Psi^i{}_{1z} C_i h_{xi} & \sum_{i=1}^{NC} \Psi^i{}_{2z} C_i h_{xi} & \cdots & \sum_{i=1}^{NC} \Psi^i{}_{Nmz} C_i h_{xi}\} \\ \frac{1}{I_{xxF}}\{-\sum_{i=1}^{NC} \Psi^i{}_{1z} C_i h_{yi} & -\sum_{i=1}^{NC} \Psi^i{}_{2z} C_i h_{yi} & \cdots & -\sum_{i=1}^{NC} \Psi^i{}_{\bar{N}mz} C_i h_{yi}\} \end{bmatrix}_{3\times Nm}
$$

$$a_{51}\Big] = [\bar{M}]^{-1}\begin{bmatrix} \sum_{i=1}^{NC}\Psi^i{}_{1z}K_i & -\sum_{i=1}^{NC}\Psi^i{}_{1z}K_ip_{xi} & \sum_{i=1}^{NC}\Psi^i{}_{1z}K_ip_{yi} \\ \sum_{i=1}^{NC}\Psi^i{}_{2z}K_i & -\sum_{i=1}^{NC}\Psi^i{}_{2z}K_ip_{xi} & \sum_{i=1}^{NC}\Psi^i{}_{2z}K_ip_{yi} \\ \vdots & \vdots & \vdots \\ \sum_{i=1}^{NC}\Psi^i{}_{Nmz}K_i & -\sum_{i=1}^{NC}\Psi^i{}_{Nmz}K_ip_{xi} & \sum_{i=1}^{NC}\Psi^i{}_{Nmz}K_ip_{yi} \end{bmatrix}_{Nm\times 3}$$

$$a_{52}\Big] = [\bar{M}]^{-1}\begin{bmatrix} -\sum_{i=1}^{NC}\Psi^i{}_{1z}K_i & \sum_{i=1}^{NC}\Psi^i{}_{1z}K_ih_{xi} & -\sum_{i=1}^{NC}\Psi^i{}_{1z}K_ih_{yi} \\ -\sum_{i=1}^{NC}\Psi^i{}_{2z}K_i & \sum_{i=1}^{NC}\Psi^i{}_{2z}K_ih_{xi} & -\sum_{i=1}^{NC}\Psi^i{}_{2z}K_ih_{yi} \\ \vdots & \vdots & \vdots \\ -\sum_{i=1}^{NC}\Psi^i{}_{Nmz}K_i & \sum_{i=1}^{NC}\Psi^i{}_{Nmz}K_ih_{xi} & -\sum_{i=1}^{NC}\Psi^i{}_{Nmz}K_ih_{yi} \end{bmatrix}_{Nm\times 3}$$

$$\left[a_{53}\right] = -[\bar{M}]^{-1}\begin{bmatrix} \sum_{i=1}^{NC}K_i\Psi^i{}_{1z}\Psi^i{}_{1z} & \sum_{i=1}^{NC}K_i\Psi^i{}_{2z}\Psi^i{}_{1z} & \cdots & \sum_{i=1}^{NC}K_i\Psi^i{}_{Nmz}\Psi^i{}_{1z} \\ \sum_{i=1}^{NC}K_i\Psi^i{}_{1z}\Psi^i{}_{2z} & \sum_{i=1}^{NC}K_i\Psi^i{}_{2z}\Psi^i{}_{2z} & \cdots & \sum_{i=1}^{NC}K_i\Psi^i{}_{Nmz}\Psi^i{}_{2z} \\ \vdots & \vdots & \vdots & \vdots \\ \sum_{i=1}^{NC}K_i\Psi^i{}_{1z}\Psi^i{}_{Nmz} & \sum_{i=1}^{NC}K_i\Psi^i{}_{2z}\Psi^i{}_{Nmz} & \cdots & \sum_{i=1}^{NC}K_i\Psi^i{}_{Nmz}\Psi^i{}_{Nmz} \end{bmatrix}_{Nm\times Nm}$$

$$-[\bar{M}]^{-1}[\bar{K}]$$

$$\left[a_{61} \right] = [\bar{M}]^{-1} \begin{bmatrix} \sum_{i=1}^{NC} \Psi^i{}_{1z} C_i & -\sum_{i=1}^{NC} \Psi^i{}_{1z} C_i p_{xi} & \sum_{i=1}^{NC} \Psi^i{}_{1z} C_i p_{yi} \\ \sum_{i=1}^{NC} \Psi^i{}_{2z} C_i & -\sum_{i=1}^{NC} \Psi^i{}_{2z} C_i p_{xi} & \sum_{i=1}^{NC} \Psi^i{}_{2z} C_i p_{yi} \\ \vdots & \vdots & \vdots \\ \sum_{i=1}^{NC} \Psi^i{}_{Nmz} C_i & -\sum_{i=1}^{NC} \Psi^i{}_{Nmz} C_i p_{xi} & \sum_{i=1}^{NC} \Psi^i{}_{Nmz} C_i p_{yi} \end{bmatrix}_{Nm \times 3}$$

$$\left[a_{62} \right] = [\bar{M}]^{-1} \begin{bmatrix} -\sum_{i=1}^{NC} \Psi^i{}_{1z} C_i & \sum_{i=1}^{NC} \Psi^i{}_{1z} C_i h_{xi} & -\sum_{i=1}^{NC} \Psi^i{}_{1z} C_i h_{yi} \\ -\sum_{i=1}^{NC} \Psi^i{}_{2z} C_i & \sum_{i=1}^{NC} \Psi^i{}_{2z} C_i h_{xi} & -\sum_{i=1}^{NC} \Psi^i{}_{2z} C_i h_{yi} \\ \vdots & \vdots & \vdots \\ -\sum_{i=1}^{NC} \Psi^i{}_{Nmz} C_i & \sum_{i=1}^{NC} \Psi^i{}_{Nmz} C_i h_{xi} & -\sum_{i=1}^{NC} \Psi^i{}_{Nmz} C_i h_{yi} \end{bmatrix}_{Nm \times 3}$$

$$\left[a_{63} \right] = -[\bar{M}]^{-1} \begin{bmatrix} \sum_{i=1}^{NC} C_i \Psi^i{}_{1z} \Psi^i{}_{1z} & \sum_{i=1}^{NC} C_i \Psi^i{}_{2z} \Psi^i{}_{1z} & \cdots & \sum_{i=1}^{NC} C_i \Psi^i{}_{Nmz} \Psi^i{}_{1z} \\ \sum_{i=1}^{NC} C_i \Psi^i{}_{1z} \Psi^i{}_{2z} & \sum_{i=1}^{NC} C_i \Psi^i{}_{2z} \Psi^i{}_{2z} & \cdots & \sum_{i=1}^{NC} C_i \Psi^i{}_{Nmz} \Psi^i{}_{2z} \\ \vdots & \vdots & \vdots & \vdots \\ \sum_{i=1}^{NC} C_i \Psi^i{}_{1z} \Psi^i{}_{Nmz} & \sum_{i=1}^{NC} C_i \Psi^i{}_{2z} \Psi^i{}_{Nmz} & \cdots & \sum_{i=1}^{NC} C_i \Psi^i{}_{Nmz} \Psi^i{}_{Nmz} \end{bmatrix}_{Nm \times Nm}$$

$$-[\bar{M}]^{-1}[\bar{C}]$$

$$\left[\ B\ \right] \quad = \quad \left[\begin{array}{c} \{0\} \\ \cdots \\ b_1 \\ b_2 \\ b_3 \end{array}\right]_{2(6+Nm)\times NC}$$

$$\left[\ b_1\ \right] \quad = \quad \left[\begin{array}{cccc} \frac{1}{m_{GB}} & \frac{1}{m_{GB}} & \cdots & \frac{1}{m_{GB}} \\ -\frac{p_{x1}}{I_{yyGB}} & -\frac{p_{x2}}{I_{yyGB}} & \cdots & -\frac{p_{xNC}}{I_{yyGB}} \\ \frac{p_{y1}}{I_{xxGB}} & \frac{p_{y2}}{I_{xxGB}} & \cdots & \frac{p_{yNC}}{I_{xxGB}} \end{array}\right]_{3\times NC}$$

$$\left[\ b_2\ \right] \quad = \quad \left[\begin{array}{cccc} -\frac{1}{m_F} & -\frac{1}{m_F} & \cdots & -\frac{1}{m_F} \\ \frac{h_{x1}}{I_{yyF}} & \frac{h_{x2}}{I_{yyF}} & \cdots & \frac{h_{xNC}}{I_{yyF}} \\ -\frac{h_{y1}}{I_{xxF}} & -\frac{h_{y2}}{I_{xxF}} & \cdots & -\frac{h_{yNC}}{I_{xxF}} \end{array}\right]_{3\times NC}$$

$$\left[\ b_3\ \right] \quad = \quad -\left[\bar{M}\right]^{-1} \left[\begin{array}{cccc} {\Psi^1}_{1z} & {\Psi^2}_{1z} & \cdots & {\Psi^{NC}}_{1z} \\ {\Psi^1}_{2z} & {\Psi^2}_{2z} & \cdots & {\Psi^{NC}}_{2z} \\ \vdots & \vdots & \vdots & \vdots \\ {\Psi^1}_{Nmz} & {\Psi^2}_{Nmz} & \cdots & {\Psi^{NC}}_{Nmz} \end{array}\right]_{Nm\times NC}$$

$$\left\{ Y \right\} = \left\{ \begin{array}{c} z_0 \\ z_1 \\ z_2 \\ \vdots \\ z_n \end{array} \right\}_{(n+1)\times 1}$$

$$\left[C \right] = \left[\begin{array}{cccccccccc:c} 1 & 0 & 0 & 0 & 0 & 0 & 0 & 0 & \cdots & 0 & \vdots & \\ 0 & 0 & 0 & 1 & -x_{F1} & -y_{F1} & \Psi^1{}_1 & \Psi^1{}_2 & \cdots & \Psi^1{}_{Nm} & \vdots & \\ 0 & 0 & 0 & 1 & -x_{F2} & -y_{F2} & \Psi^2{}_1 & \Psi^2{}_2 & \cdots & \Psi^2{}_{Nm} & \vdots & \{0\} \\ \vdots & \vdots & \vdots & \vdots & \vdots & \vdots & \vdots & \vdots & \vdots & \vdots & \vdots & \\ 0 & 0 & 0 & 1 & -x_{Fn} & -y_{Fn} & \Psi^{Nm}{}_1 & \Psi^{Nm}{}_2 & \cdots & \Psi^{Nm}{}_{Nm} & \vdots & \end{array} \right]_{(n+1)\times 2(6+Nm)}$$

x_{Fi} and y_{Fi} $(i = 1, 2...n)$ represent the coordinates of the i-th node from centre of mass of the fuselage. The vector $\{Y\}_s$ and the matrix $[C_s]$ corresponding to the preselected sensor locations are subsets of the vector$\{Y\}$ and matrix [C] respectively, given above.

Appendix B

Definition of condition number

The quantity $\|A\| \, \|A^{-1}\|$ is defined as the Condition number of a nonsingular square matrix A (Ref.41) and will be denoted as Cond (A). In the present study, the condition number is defined based on infinity norm of matrix A.

The infinity norm of a general matrix A of size $m \times n$ is defined as

$$\|A\|_\infty = \max_{1 \le i \le m} \left(\sum_{j=1}^{n} |a_{ij}| \right)$$

Appendix C

Helicopter model as two degrees of freedom system

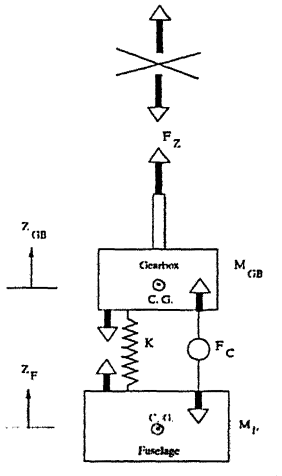

The equations of motion of the two degrees of freedom system can be written as

$$M_{GB}\ddot{Z}_{GB} + K(Z_{GB} - Z_F) = F_Z + F_C$$

$$M_F\ddot{Z}_F + K(Z_F - Z_{GB}) = 0 - F_C$$

Writing the equations in matrix form,

$$\begin{bmatrix} M_{GB} & 0 \\ 0 & M_F \end{bmatrix} \begin{Bmatrix} \ddot{Z}_{GB} \\ \ddot{Z}_F \end{Bmatrix} + \begin{bmatrix} K & -K \\ -K & K \end{bmatrix} \begin{Bmatrix} Z_{GB} \\ Z_F \end{Bmatrix} = \begin{Bmatrix} F_Z + F_C \\ -F_C \end{Bmatrix}$$

Assuming the harmonic input $F_Z = \bar{F}_Z e^{i\omega t}$, the response and the control force can be written as,

$$Z_{GB} = \bar{Z}_{GB}e^{i\omega t}, Z_F = \bar{Z}_F e^{i\omega t}, F_C = \bar{F}_C e^{i\omega t}$$

Substituting the soultion in the equations, the amplitude of the response can be obtained from the following relation.

$$\begin{bmatrix} K - M_{GB}\omega^2 & -K \\ -K & K - M_F\omega^2 \end{bmatrix} \begin{Bmatrix} \bar{Z}_{GB} \\ \bar{Z}_F \end{Bmatrix} = \begin{Bmatrix} \bar{F}_Z + \bar{F}_C \\ -\bar{F}_C \end{Bmatrix}$$

The response can be written as

$$\begin{Bmatrix} \bar{Z}_{GB} \\ \bar{Z}_F \end{Bmatrix} = \frac{1}{M_{GB}M_F\omega^4 - K\omega^2(M_{GB} + M_F)} \begin{bmatrix} K - M_F\omega^2 & K \\ K & K - M_{GB}\omega^2 \end{bmatrix} \begin{Bmatrix} \bar{F}_Z + \bar{F}_C \\ -\bar{F}_C \end{Bmatrix}$$

$$\bar{Z}_{GB} = \frac{(K - M_F\omega^2)\bar{F}_Z - M_F\omega^2\bar{F}_C}{M_{GB}M_F\omega^4 - K\omega^2(M_{GB} + M_F)}$$

and,

$$\bar{Z}_F = \frac{K\bar{F}_Z + M_{GB}\omega^2\bar{F}_C}{M_{GB}M_F\omega^4 - K\omega^2(M_{GB} + M_F)}$$

Thus,

$$Z_{GB} = \bar{Z}_{GB}e^{i\omega t}$$

$$Z_F = \bar{Z}_F e^{i\omega t}$$

The fuselage response Z_F will be zero, if

$$\bar{F}_C = -\frac{K}{M_{GB}\omega^2}\bar{F}_Z$$

The negative sign in the above equation indicates that F_C must be out-of-phase (180 degrees) to the input force F_Z